의학박사 학위논문

The functional role of phosphatase Ssu72 in alveolar macrophages

탈인산가수분해효소 Ssu72의 폐포대식세포 발달 및 기능에 관한 연구

2019 년 8 월

서울대학교 대학원

의과학 전공

우 연 덕

의학박사 학위논문

탈인산가수분해효소 Ssu72의 폐포대식세포 발달 및 기능에 관한 연구

The functional role of phosphatase Ssu72 in alveolar macrophages

2019 년 8 월

서울대학교 대학원

의과학 전공

우 연 덕

The functional role of phosphatase Ssu72 in alveolar macrophages

지도교수 정 두 현

이 논문을 의학박사 학위논문으로 제출함

2019년 8월

서울대학교 대학원

의과학 전공

우 연 덕

우연덕의 의학박사 학위논문을 인준함

2019년 8월

위 원 장 _____ (인)

부 위 원 장 _____ (인)

위 원 _____ (인)

위 원 _____ (인)

위 원 _____ (인)

Abstract

The functional role of Ssu72 in alveolar macrophages

우연덕 (Yeon Duk Woo)

의과학과 (Biomedical Science)

의과학 전공 (Major in Biomedical Science)

Seoul National University, Graduate School

Ssu72 phosphatase was originally identified for its role in regulation of RNA Polymerase II (RNAP-II) activity by directly regulating phosphorylation of serine and tyrosine residues of C-terminal domain of RANP-II. However, the function of Ssu72 phosphatase is expanding. Recent reports suggest different functional roles of Ssu72 in different cell types suggesting that Ssu72 might be involved in many cellular processes and molecular pathways. For example, Ssu72 regulates hepatocyte cell cycle by directly regulating phosphorylation of Retinoblastoma protein. Moreover, Ssu72 regulated development of arthritis by regulating Th17 cell differentiation and function. Based on these recent reports, Ssu72 might play key roles in other cells types including those of macrophages. *Lysm*-Cre*Ssu72*$^{fl/fl}$ mice was used to study the functional role of Ssu72 in macrophages, and surprisingly, Ssu72 was found to regulate lung resident alveolar macrophage (AM) development and maturation but not

those of any other macrophages. Using *Cd11c*-cre*Ssu72*$^{fl/fl}$ mice, AM precursors were traced from embryonic stages, which showed that Ssu72 regulated development and maturation of AMs from neonatal stages of mice. Mechanism wise, Ssu72 was rapidly induced upon Granulocyte macrophage-colony stimulating factor (GM-CSF) stimulation in AMs and upon GM-CSF stimulation, Ssu72 directly bound to GM-CSF receptor β chain (GM-CSFR βc). Moreover, GM-CSF increased phosphorylation of GM-CSFR βc and downstream molecules, and induced dysregulations in cell cycle, death, and mitochondrial respiration in mature Ssu72-deficient AMs compared with those of mature WT AMs. The dysregulations found in mature Ssu72-deficient AMs were restored by treatment with AZD1480, which restored GM-CSFR βc phosphorylation in mature Ssu72-deficient AMs like that of mature WT AMs. Furthermore, *Lysm*-Cre*Ssu72*$^{fl/fl}$ mice failed to develop allergic asthma, which Ssu72-deficient AMs were directly responsible for. Combined, these results demonstrate the critical role of Ssu72 in regulation of GM-CSF signaling by binding to and regulating phosphorylation of GM-CSFR βc, thereby contributing to the development and maturation of AMs.

Keywords: Ssu72, Alveolar macrophages, GM-CSF, fine-tuning

***Student number**: 2013-21780*

CONTENTS

LIST OF FIGURES

LIST OF MAJOR ABBREVIATIONS AND SYMBOLS

AM : Alveolar macrophage

IM : Interstitial macrophage

BMDM : Bone-marrow derived macrophage

GM-CSF : Granulocyte-macrophage colony-stimulating factor

M-CSF : Macrophage colony-stimulating factor

PAP : pulmonary alveolar proteinosis

GM-CSFR : GM-CSF receptor

GM-CSFR βc : GM-CSF receptor beta chain

GM-CSFR αc : GM-CS receptor alpha chain

Ssu72 : SSU72 Homolog, RNA Polymerase II CTD Phosphatase

INTRODUCTION

Current studies on origin and development of tissue resident macrophages have countered the long-held belief on monocyte derived origin of macrophages[1]. Recently, it has been reported that the progenitor cells of tissue resident macrophages move into target tissues at early embryonic stages of life and differentiate into tissue resident macrophages with minimal contribution from monocytes[2]. Studies using $CCR2^{-/-}$ mice[3, 4], which blocks monocyte infiltration into tissues or parabiosis experiments[5] have shown relatively little monocyte contribution in formation of tissue resident macrophages under steady state or under inflammation. These tissue resident macrophage subsets differentially exhibit gene-expression profiles and transcriptional pathways from each other as well as from bone-marrow derived macrophages (BMDMs) which has been traditionally used to study macrophages, suggesting that unique cellular pathways might be responsible for the development and maturation of individual tissue resident macrophage in various tissues[6]. One of the key features of tissue resident macrophages is that they have the ability to self-renew in the differentiated state.[7] Although the cytokines and transcription factors responsible for development of tissue resident macrophages have been

studied to some degree, the detailed molecular mechanisms by which these cells self-renew is yet to be fully discovered. In addition, the complex signaling events within different tissues further suggest different molecular mechanisms may be at hand for regulation of different tissue resident macrophages.[8]

Among tissue resident macrophages, the development of AM is unique in that this subset of macrophage mainly depends on cytokine GM-CSF for its development [9, 10, 11] while most of the other tissue resident macrophages depend upon Macrophage colony-stimulating factor (M-CSF)[2]. Based on these evidences, one can hypothesize that unique molecular mechanisms may be regulating AM development and maturation. The importance of GM-CSF in AM development has been studied in detail. GM-CSF gene ablation induced multiple abnormalities in AMs accompanied by pulmonary alveolar proteinosis (PAP), whereas marked elevation of GM-CSF levels in the lungs develops alveolar type II cell hyperplasia via progressive alveolar macrophage accumulation[12]. In addition, deletion of GM-CSF receptor signaling abolishes AM development altogether. Moreover, GM-CSF-mediated induction of transcription factor PPAR-γ plays critical role in the differentiation of fetal monocytes into alveolar macrophages within the first week of life, thereby establishing GM-CSF-PPAR-γ axis in the development of AMs [10]. *In-vitro* studies have demonstrated that different kinases are involved

in regulating phosphorylation of tyrosine or serine residues on GM-CSF receptor (GM-CSFR) that determines the cellular fates in response to GM-CSF [13]. In GM-CSFR signaling, kinase PKA and JAK2 are responsible for phosphorylation on serine and tyrosine residues on GM-CSFR, respectively. Furthermore, signaling is regulated via balancing between positive and negative signals [14], thereby providing fine-tuning of GM-CSFR signaling. Based on function of phosphatase as an enzyme for de-phosphorylation of target molecules, it is reasonable to consider that phosphatase might be a possible regulator for fine-tuning of GM-CSFR signaling by negatively balancing GM-CSFR signaling in AMs. However, there has been no study to report phosphatase that regulates GM-CSFR signaling in such manner.

Ssu72 is a phosphatase first identified as regulator of RNA Polymerase II (RNAP-II) activity in the nucleus [15]. Ssu72 was found to directly bind to C-terminal domain (CTD) of RNAP-II and eliminate phosphorylation of tyrosine and serine residues on CTDs in yeast and mammalian cells, which enables RNAP-II to be recycled [16]. Very recently, Ssu72 phosphatase was found to directly bind to Aurora B kinase in HeLa cells and Rb protein in hepatocytes, thereby regulating cell cycle [17]. These findings indicate that Ssu72 exerts RNAP-II-independent phosphatase activity in different cellular events. In addition, in the field of immunology, Ssu72 phosphatase was found to attenuate autoimmune

arthritis by regulating STAT3 signaling and Th17 activation[18]. This study is the first report demonstrating the functional role of Ssu72 phosphatase in the field of immunology. Nevertheless, the function of Ssu72 in tissue-resident macrophages has not been reported yet.

To address this, *Lysm*-Cre*Ssu*72$^{fl/fl}$ mice was generated by crossing *Lysm*-Cre transgenic mice with *Ssu72*$^{fl/fl}$ mice. *Lysm*-Cre*Ssu*72$^{fl/fl}$ mice showed defects in development and maturation of lung resident AMs but not in any other myeloid cell subsets. Ssu72 deficient AMs exhibited a dysregulation of death, cell cycle, and mitochondrial respiration upon GM-CSF stimulation, which was restored by reducing GM-CSFR signaling strength using JAK2 inhibitor. Furthermore, tracing of AM precursors using *Cd11c*-cre*Ssu72*$^{fl/fl}$ mice exhibited a defect in the development and maturation of AMs postnatally. Co-immunoprecipitation assay revealed that in presence of GM-CSF, Ssu72 directly bound to GM-CSFR βc which is a signal transducing chain of GM-CSFR and regulated GM-CSFR βc phosphorylation thereby regulating GM-CSFR signaling altogether. Lastly, *Lysm*-Cre*Ssu*72$^{fl/fl}$ mice failed to develop allergic asthma which was restored by adoptive transfer of WT mature AMs or JAK2 inhibitor treated *Lysm*-Cre*Ssu72*$^{fl/fl}$ mature AMs. In conclusion, these results demonstrate that Ssu72 phosphatase fine-tunes GM-CSFR signaling by binding to and regulating phosphorylation of GM-CSFR βc, thereby contributing to the

development and maturation of AMs.

MATERIALS AND METHODS

Mice.

Lysm-Cre and *Cd11c*-Cre mice were purchased from the Jackson laboratory. *Lysm*-Cre mice were crossed to *Ssu72*$^{fl/fl}$ to generate mice with deficiency in Ssu72 in *lyz2* expressing cells. *Cd11c*-Cre mice were crossed to *Ssu72*$^{fl/fl}$ to generate mice with deficiency in Ssu72 in *itgax* expressing cells. All experiments were conducted between ages of 8 to 10 weeks unless otherwise noted. All experiments were approved by the Institutional Animal Care and Use Committee in Seoul National University Hospital (SNUH-IACUC) and animals were maintained in the facility accredited AAALAC International (#001169) in accordance with Guide for the Care and Use of Laboratory Animals 8th edition.

Quantitative real-time PCR.

Total RNA was isolated using TRIzol reagent (Invitrogen) according to the manufacturer's protocol. RNA was reversely transcribed into cDNA constructs using Maloney murine leukemia virus reverse transcriptase Taq polymerase (Promega). For quantitative RT-PCR, gene specific PCR products were quantified using an Applied Biosystems 7500 Sequence Detection System (Applied Biosystems). Expression levels were normalized to that of gapdh, calculated by the delta-delta Ct method.

Primer sequences used are enlisted in Table 1.

Single cell suspension preparations.

Peritoneal lavages were performed by injecting 5 ml 1× PBS into mice peritoneum and harvesting the fluids. Spleens were treated with RBC lysis solution while being minced and passed through 40μm cell strainer. Brains were digested for 30 min at 37°C in type IV collagenase containing medium and passed through a 40- m cell strainer. Cells were re-suspended in 30% Percoll layered over 70% Percoll (GE Healthcare) before density centrifugation at 2000 rpm for 25 min at 25°C. The interphase was collected using transfer pipettes and was used for further analysis. The lungs were digested for 1 hour at 37°C with type IV collagenase and were passed through a 40μm cell strainer while treated with RBC lysis solution. Livers were digested in type IV collagenase for 30 min at 37°C. Liver cell suspensions were centrifuged at 2,000 rpm for 15 min in 33% Percoll density centrifugation followed by treatment with RBC lysis solution. BAL fluid was isolated by canalization of the trachea with a catheter. The lungs were flushed three times with 1 mL 1× PBS, and harvested cells were used for further analysis.

Flow cytometry

LSR Fortessa (BD) was used for multi-parameter analysis, and data were

analyzed with FlowJo software (Treestar). The antibodies used in the experiments are enlisted in Table 2. Prior to all staining, FCγIII/II receptors were blocked by incubation with anti-CD16/32 antibodies for 15 min at 4°C.

Hematoxylin & Eosin and Oil Red O staining

Cytospins of BAL fluid cells or flow cytometry-sorted AMs (BD Aria III) were fixed for 10 minutes with 4% formalin, washed twice with 1× PBS. For H&E staining, samples were stained with hematoxylin for 40 seconds followed by staining with eosin for 30 seconds. The samples were examined under a light microscope after mounting with mounting medium. For Oil Red O staining, the samples were stained for 30 minutes with a 0.5% Oil Red O in 60% isopropanol, followed by 2 min of de-staining and washing with 1× PBS. Nuclei were subsequently stained with hematoxylin.

Analysis and genotyping of embryos.

Heterozygous mouse breeding pairs were monitored daily for vaginal plugs. Between embryonic days of 17.5 – 21.5, uteruses were isolated from plugged females. DNAs isolated from embryo tails were used for genomic DNA PCR to determine genotypes.

Immunoprecipitation and immunoblotting.

For immunoprecipitations, the cell lysates were prepared by treating lysis buffer containing Tris-Cl (pH 7.9, 20 mM), NaCl (120 mM), Triton X-100 (0.5%), EDTA (2.5 mM), and DTT (2 mM) in presence of protease and phosphatase inhibitor cocktails (Gendepot) to samples. The eluted samples were loaded onto 8% ~ 12% SDS-PAGE gels and transferred onto a polyvinylidene fluoride membrane (Millipore) for immunoblotting. The antibodies used for immunoblotting is listed in table 3.

Preparation of nucleus and cytosolic fraction of cells.

Buffer A (10 mM HEPES, pH 7.9, 10 mM KCl, 0.1 mM EDTA, 0.1 mM EGTA, 1 mM DTT, and protease inhibitor cocktail) and Buffer B (20 mM HEPES, pH 7.9, 400 mM NaCl, 1 mM EDTA, 1mM EGTA, 1 mM DTT and protease inhibitor cocktail) were used to separate cytosolic fraction from nuclear fraction. Buffer A was treated first to the samples followed by centrifugation at 13,000 rpm for 5 min at 4°C. Supernatants were harvested and used as cytoplasm fractions. The remaining pellets were re-suspended in Buffer B and centrifuged at 13,000 rpm for 5 minutes at 4°C. Supernatants were harvested and used as nuclear fractions.

Co-immunoprecipitation.

The cell lysates were harvested using lysis buffer followed by incubation with immunoprecipitation antibodies for 4 h at 4°C on a rotator. Lysates were further treated with agarose beads overnight at 4°C on a rotator and proceeded for washing before immunoblotting.

Cell sorting for AMs and fetal monocytes

BAL fluid cells and the lungs were obtained from *Lysm*-Cre and *Lysm*-Cre*Ssu*72$^{fl/fl}$ mice, stained with various antibodies, and sorted for mature CD45^{+}CD11c^{+}F4/80^{+}Siglec-F^{+}CD11b^{-} AMs or CD45^{+}CD11c^{+}F4/80^{+} fetal monocytes using BD ARIA III.

Microarray Analysis.

Total RNA of sorted mature AMs from lungs of 8 - 10 week-old mice was isolated using TRIzol reagent and amplified and hybridized on an Affymetrix Mouse Gene 1.1 ST array. Heat maps were visualized with MultiExperiment Viewer software. Pathway analysis was performed with MetaCore software and pathway mapping by the KEGG database.

Cell cycle analysis and measurement of antigen uptake by AMs

Vybrant cell cycle dye (Invitrogen) was used according to the manufacturer's instructions. For measurement of antigen uptake, mature

AMs were pulsed with 50 μg of FITC-tagged OVA (Invitrogen) or untagged OVA (Sigma) for 4 h at 37°C and intracellular fluorescence in AMs were analyzed using flow cytometry.

***In vitro* AM & fetal monocytes culture and AZD 1480 treatment.**

Mature AMs and fetal monocytes were cultured in complete RPMI (constitutes 10% FBS, 1% Penicillin & Streptomycin, 1% HEPES, 1% Non-Essential Amino Acid, 1% Sodium Pyruvate and 1% 2-ME) in presence of GM-CSF (20 ng/ml for mature AMs and 50 ng/ml for fetal monocytes). Mature AMs were pretreated with AZD 1480 (2 μM) for 2 h, washed with 1× PBS twice, and used for experiments.

Measurement of extracellular acidification rate (ECAR) and oxygen consumption rate (OCR)

Approximately 2 x 10^5 mature AMs were plated per well of XF24 cell culture microplates (Seahorse Bioscience) to analyze ECAR and OCR. For the ECAR measurement, mature AMs were sequentially treated with glucose (10 mM), oligomycin (1 μM), and 2-DG (50 mM), whereas oligomycin (1 μM), FCCP (1 μM), Rotenone (1 μM), and antimycin A (1 μM) were added to mature AMs to estimate OCR. (C and D) Areas under the curve (AUC) for ECAR (C) and OCR (D) in the mature WT and Ssu72-deficient AMs were calculated and compared. The acquired

data were normalized to the total protein concentrations, which were measured by the standard Bradford assay.

Mitochondrial staining in AMs

Sorted mature AMs or total BAL fluid cells were stained with MitoSox (1μM), MitoTracker-Orange CMTM (100 nM), and MitoTracker Green (100 nM) for estimating mitochondria ROS, mitochondrial membrane potential, and mitochondrial mass, respectively according to manufacturer's protocol (Thermo Fisher Scientific). These parameters were measured using flow cytometry. In case of BAL fluid cells, AMs were gated and estimated in flow cytometry.

***In vivo* experiments using BrdU**

Lysm-Cre mice and *Lysm*-Cre*Ssu72*$^{fl/fl}$ mice were injected daily with 1 mg BrdU (Sigma) for 3 weeks. 1 day and 21 days after the last injection, mice were sacrificed, and BAL mature AMs were analyzed for their BrdU incorporation via flow cytometry.

Induction of OVA-induced asthma and measurement of AHR.

OVA antigen (Sigma) was dissolved in saline to 1mg/ml A combination of 4mg of aluminum hydroxide (Thermo Scientific) mixed with 100 μl of OVA in saline solution was given to C57BL/6 background mice

intraperitoneally at day 0 and 7, respectively. 50 μg of OVA solution (1mg/ml) was delivered intranasally to isoflurane-anesthetized mice on days 14, 15, 16, and 17. 2.0 x 10^5 mature AMs from *Lysm*-Cre or *Lysm*-Cre*Ssu*72$^{fl/fl}$ mice were dissolved in 50 μl of 1× PBS and administered to *Lysm*-Cre*Ssu*72$^{fl/fl}$ mice on days 13 and 15 via intratracheal route. 24 h after the final intranasal instillation, AHR was measured in response to increasing doses of methacholine (0, 5, 10, 20, and 40 mg/ml) using the forced oscillation technique (Flexivent System). A "snapshot perturbation" maneuver was imposed to measure the resistance (R) of the whole respiratory system.

Preparation of Bone-Marrow Derived Macrophages.

The mouse BMDMS were prepared from the femurs and tibias of 8 to 10 week-old mice. Each femurs and tibias were flushed with 1 1× PBS twice followed by treatment with RBC lysis solution. Bone marrow cells were cultured with DMEM supplemented with 10% FBS, 1% penicillin & streptomycin, and mouse recombinant M-CSF (20 ng/ml). Fresh M-CSF and growth media were added on day 3. Between days 6 - 8, adherent cells were harvested and used for any further experiments. The purity of BMDMs were measured by F4/80 and CD11b expression via flow cytometry.

Immunofluorescence Using Confocal Microscopy

Confocal fluorescent images were obtained by a Zeiss LSM510NL confocal scan head on an inverted-based microscope with a 63x objective. Sequential excitation at 488 nm and 543 nm was provided by argon and helium-neon gas lasers, respectively. Emission filters BP500-550 was used for collecting green in channel one. After excitation, green fluorescent images of the same cells were saved and processed for further analysis.

Enzyme-linked immunosorbent assay (ELISA)

Total protein concentrations in BAL fluid were measured by Bradford assay according to the manufacturer's instructions (Bio-Rad). For measurement of SP-D, wells were coated with 0.25 μg/ml (1:4,000 dilution) polyclonal rabbit antibody to mouse SP-D (LS-C17965; LIFESPAN Biosciences), followed by detection with 2 μg/ml biotinylated monoclonal antibody to mouse SP-D (VIF11;Abcam). To measure GM-CSF levels in lungs, BD Bioscience ELISA Kit was used according to the manufacturer's protocols.

Statistical Analysis.

Statistical analysis was performed using the Prism software (version 8.0). Comparisons of two groups were calculated with the nonparametric

Mann–Whitney test. *P* value <0.05 was considered as statistically significant.

Table 1. List of real-time PCR primers

Primers for qRT-PCR		
ssu72	F	5’-CATGGAAGCACACAACATCCTCA-3’
	R	5’-TGGACGGGGCTTGATCCTTTTAT-3’
bak1	F	5’-ATATTAACCGGCGCTACGAC-3’
	R	5’-AGGCGATCTTGGTGAAGAGT-3’
bax	F	5’-TAGCAAACTGGTGCTCAAGG-3’
	R	5’-TCTTGGATCCAGACAAGCAG-3’
puma	F	5’-ATGGCCCGCGCACGCCAGG-3’
	R	5’-CCGCCGCTCGTACTGCGCGTTG-3’
bim	F	5’-CGACAGTCTCAGGAGGAACC-3’
	R	5’-CCTTCTCCATACCAGACGGA-3’
bcl2	F	5’-CTCGTCGCTACCGTCGTGACTTCG-3’
	R	5’-CAGATGCCGGTTCAGGTACTCAGTC-3’
bcl-xl	F	5’-TGGAGTAAACTGGGGGTCGCATCG-3’
	R	5’-AGCCACCGTCATGCCCGTCAGG-3’
ccnd1	F	5’-AGGAGCTGCTGCAAATGGAA-3’
	R	5’-AGGCTTGACTCCAGAAGGGC-3’
ccne1	F	5’-ACTCGACGGACCACAGCAAC-3’
	R	5’-GGGATGAAAGAGCAGGGGTC-3’
ccna2	F	5’-TTCAGCTTGTAGGCACGGCT-3’
	R	5’-CAAGTGGAAGGCAGCTCCAG-3’
ccnb1	F	5’-ACAGCTGGTCGGTGTAACGG-3’
	R	5’-TCAGCGCTAAGCAGAAAGCC-3’
cyp4a12b	F	5’-CTTCATCACAACCCAACTG-3’
	R	5’-TCTTGTTCTGTGAAGATTATT-3’
gpd1	F	5’-CTGAAGGACCTGATGCAG AC-3’
	R	5’- GCTCAATGGACTTTCCAGTTC-3’

cybb	F	5’- ACTCCTTGGGTCAGCACTGG -3’
	R	5’- GTTCCTGTCCAGTTGTCTTCG -3’
nudfb7	F	5’- GGAAGATGAGGAGGAAGATGTC -3’
	R	5’- CAGGAAGGAGAGCAGATGAAAT -3’
hpgd	F	5’- TCTACGCAGCACTGAATCCG -3’
	R	5’- GCCCTCGAACTGGGAAGTAG -3’
yy1	F	5’- CAGAAGCAGGTGCAGATCAGACCCT -3’
	R	5’- GCACCACCACCCACGGAATCG -3’
ulk1	F	5’- CACTGCGTGGCTCACCTAAG -3’
	R	5’-ACAGTTCAGCCATCACTTGGA-3’
vdac1	F	5’- AATGACGGGACAGAGTTTGG -3’
	R	5’- CCATCACAATGCCTGTGGTA -3’
tfam	F	5’- GCTCTACACGCCCCTGGTTTCTGG -3’
	R	5’- TCGCTGTAGTGCCTGCTGCTCCTG -3’
ppargc1b	F	5’- CTTGCTAACATCACAGAGGATATCTTG-3’
	R	5’- GGCAGGTTCAACCCCGA -3’
nrf1	F	5’- TATGGCGGAAGTAATGAAAGACG -3’
	R	5’- CAACGTAAGCTCTGCCTTGTT -3’
ndufs8	F	5’- TGGCGGCAACGTACAAGTAT-3’
	R	5’- CCTCGGATGAGTTCTGTCCA-3’
shda	F	5’- GAAAGGCGGGCAGGCTCTC-3’
	R	5’- CACCAGGCACTCCCCATTTT-3’
cox5a	F	5’- TTGATGCCTGGGAATTGCGTAAAG-3’
	R	5’- AACAACCTCCAAGATGCGAACAG-3’
apt5l	F	5’- GAGAAGGCACCGTCGATGG-3’
	R	5’- ACACTCTGAATAGCTGTAGGGAT-3’
il4	F	5’- TCA ACC CCC AGC TAG TTG TC -3’
	R	5’- TGT TCT TCG TTG CTG TGA GG -3’

ifng	F	5’- CGG CAC AGT CAT TGA AAG CCT A -3’
	R	5’- GTT GCT GAT GGC CTG ATT GTC -3’
il13	F	5’- CCTGGCTCTTGCTTGCCTT-3’
	R	5’- GGTCTTGTGTGATGTTGCTCA-3’
il17	F	5’- GGT CTT GTG TGA TGT TGC TCA -3’
	R	5’- GGG TCT TCA TTG CGG TGG AGA G -3’
il10	F	5’- AACATACTGCTAACCGACTCCT-3’
	R	5’- CTGCCTTGCTCTTATTTTCACA-3’
gata3	F	5’- GGAAACTCCGTCAGGGCTA -3’
	R	5’- AGAGATCCGTGCAGCAGAG -3’
tbx21	F	5’- TTCCCATTCCTGTCCTTCAC -3’
	R	5’- CCACATCCACAAACATCCTG -3’
rorc	F	5’- TGA GGC CAT TCA GTA TGT GG -3’
	R	5’- CTT CCA TTG CTC CTG CTT TC -3’
foxp3	F	5’- CCC AGG AAA GAC AGC AAC CTT -3’
	R	5’- TTC TCA CAA CCA GGC CAC TTG -3’
gapdh	F	5’- GGGAAGCTCACTGGCATGG-3’
	R	5’- CTTCTTGATGTCATCATACTTGGCAG-3’

Table 2. List of reagents used for flow cytometry

Antibody/Reagent	Catalogue #	Clone	Company
PerCP/Cyanine5.5 anti-mouse CD45	103132	30-F11	BioLegend
PE/Cy7 anti-mouse CD11c	117318	N418	BioLegend
APC anti-mouse F4/80	123116	BM8	BioLegend
PE anti-mouse/human CD11b	101208	M1/70	BioLegend
FITC anti-mouse F4/80	123108	BM8	BioLegend
PE anti-mouse CD170 (Siglec-F)	155506	S17007 L	BioLegend
Brilliant Violet 421™ anti-mouse/human CD11b	101236	M1/70	BioLegend
PE – Annexin V	640947	-	BioLegend
7-AAD viability staining solution	420404	-	BioLegend
PE/Cy7 anti-mouse Ki-67	652426	16A8	BioLegend
APC anti-mouse TNF-α	506308	MP6-XT22	BioLegend
PE anti-mouse H-2	125505	M1/42	BioLegend
PE anti-mouse I-A/I-E	107607	M5/114 .15.2	BioLegend
BV421 anti-mouse I-A/I-E	107632	M5/114 .15.2	BioLegend
APC anti-mouse CD86	105012	GL-1	BioLegend
FITC anti-mouse CD80	104706	16-10A1	BioLegend
PE anti-mouse CD274 (B7-H1, PD-L1)	124308	10F.9G 2	BioLegend
PE anti-mouse CD273 (B7-DC, PD-L2)	107206	TY25	BioLegend
FITC anti-mouse Ly-6G	127606	1A8	BioLegend
APC – CD103	121414	2E7	BioLegend
PE/Cy7 anti-mouse TCR β chain Antibody	109222	H57-597	BioLegend
PE anti-mouse CD19	152408	1D3/CD19	BioLegend
APC anti-mouse CD4	100516	RM4-5	BioLegend
FITC anti-mouse CD8a	100706	53-6.7	BioLegend
PE anti-mouse FOXP3	126404	MF-14	BioLegend
MitoSOX™ Red	M36008	-	ThermoFish

Mitochondrial Superoxide Indicator, for live-cell imaging			er Scientific
MitoTracker™ Green FM	M7514	-	ThermoFisher Scientific
MitoTracker™ Orange CM-H2™Ros	M7511	-	ThermoFisher Scientific
Ovalbumin, Fluorescein Conjugate	O23020		ThermoFisher Scientific
Mouse GM-CSFR α APC-conjugated	698423	-	R&D Biosystems
PE Rat Anti-Mouse CD131	559920	JORO50	BD Biosciences
PBS 57 – APC conjugated anti-mouse CD1d tetramer	-	-	NIH Tetramer Facility
VybrantTM DyeCycle Orange Stain	V35005	-	Invitrogen

PerCP - Peridinin-Chlorophyll-protein

PE - Phycoerythrin

PE/Cy7 – Phycoerthrin/Cyanine7

APC – Allophycocyanin

FITC - Fluorescein isothiocyanate

Table 3. List of antibodies used for immunoblotting & immunoprecipitation

Antibody/Reagent	Catalogue #	Concentration	Company
GM-CSFR βc	bs-3689R	1:500	Bioss
β-Actin	bs-0061R	1:2000	Bioss
α-Tubulin	bs-11313R	1:2000	Bioss
JAK2	sc-390539	1:1000	Santa Cruz
STAT5	sc-74442	1:1000	Santa Cruz
Phospho-Serine	9631s	1:1000	Cell Signaling Technology
Phospho-Tyrosine	9416	1:1000	Cell Signaling Technology
Ssu72	12816s	1:1000	Cell Signaling Technology
Phospho-JAK2	3711s	1:500	Cell Signaling Technology
Phospho-STAT5	9351s	1:1000	Cell Signaling Technology
Phospho-P38	4511s	1:1000	Cell Signaling Technology
P38	8690s	1:1000	Cell Signaling Technology
Phospho-AKT	4060s	1:1000	Cell Signaling Technology
AKT	4691s	1:1000	Cell Signaling Technology

Phospho-MEK1/2	9121s	1:1000	Cell Signaling Technology
MEK1/2	9122s	1:1000	Cell Signaling Technology
Phospho-ERK1/2	4370s	1:1000	Cell Signaling Technology
ERK1/2	4695s	1:1000	Cell Signaling Technology
Phospho-JNK1/2	9251s	1:1000	Cell Signaling Technology
JNK1/2	9252	1:1000	Cell Signaling Technology

JAK2 – Janus kinase 2

STAT5 – Signal transducer and activator of transcription 5

P38 – P38 mitogen-activated protein kinases

AKT – Protein kinase B

MEK1/2 – Mitogen-activated protein kinase kinase 1/2

ERK1/2 – Extracellular signal-regulated kinases 1/2

JNK1/2 – c-Jun N-terminal kinase 1/2

RESULTS

Ssu72 expression in various immune cell subsets

To explore whether Ssu72 phosphatase plays a role in immune cells, *ssu72* expression was measured in various immune cell subsets sorted from spleens of wild-type (WT) mice. Among immune cell subsets analyzed, T lymphocytes and macrophages were two subsets with the highest *ssu72* expression. *Ssu72* expression in macrophages was at least two times higher than those of other innate immune cells analyzed (neutrophils, eosinophils, macrophages and dendritic cells (DCs)). (Figure 1) As mentioned briefly in introduction, the function of Ssu72 in T lymphocytes is already reported, therefore the focus of this study was to investigate a possible role of Ssu72 in macrophages.

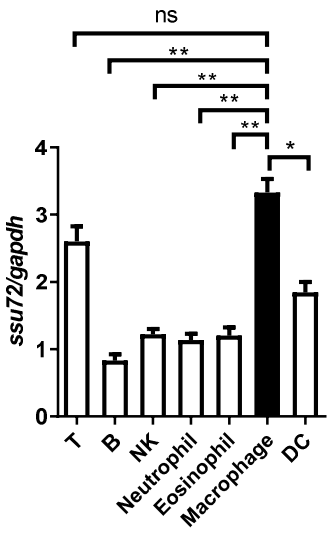

Figure 1. *ssu72* expression in various immune cell subsets.

Immune cell subsets were sorted from spleens of naïve C57BL/6 wild-type (WT) mice via flow-cytometry and their relative *ssu72* expressions were compared via real-time PCR. Expression levels are represented as a fold change over the expression in neutrophils. The following markers were used to gate and sort immune cell subsets. (T – $TCR\beta^{+}CD19^{-}$, B – $TCR\beta^{-}CD19^{+}$, NK – $TCR\beta^{-}NK1.1^{+}$, Neutrophil – $CD11b^{+}Ly6G^{+}$, Eosinophil – $CD11b^{+}Siglec\text{-}F^{+}$, Macrophage – $F4/80^{+}$ Dendritic Cells (DC) – $CD11c^{+}MHC\text{-}II^{+}$) ($n$ = 5). Data were pooled from 3 independent experiments and presented as means ± standard error of the means (SEMs). Ns, Not significant. *P<0.5, **P<0.01, and ***P<0.001.

Analysis of *Lysm*-Cre*Ssu72*$^{fl/fl}$ mice

To investigate the functional role of Ssu72 in macrophages, *Ssu72*$^{fl/fl}$ mice was crossed to *Lysm*-Cre transgenic mice to generate *Lysm*-Cre*Ssu72*$^{fl/fl}$ mice. Though these mice were generated to study the function of Ssu72 in macrophages, circulating monocytes, neutrophils and eosinophils were also analyzed because they also express *lyz2* which encodes Lysm. The comparative analysis of monocytes, neutrophils, and eosinophils of *Lysm*-Cre and *Lysm*-Cre*Ssu72*$^{fl/fl}$ mice via flow-cytometry revealed similar percentages and numbers throughout different tissues. (Figure 2A) In addition, these cells were sorted from *Lysm*-Cre and *Lysm*-Cre*Ssu72*$^{fl/fl}$ mice via flow cytometry and measured for their *ssu72* expression via real-time PCR. Real-time PCR results confirmed successful deletion of *ssu72* in the cells sorted from *Lysm*-Cre*Ssu72*$^{fl/fl}$ mice while the level of *ssu72* expression was similar between T cells sorted from spleens of *Lysm*-Cre and *Lysm*-Cre*Ssu72*$^{fl/fl}$ mice. (Figure 2B &C)

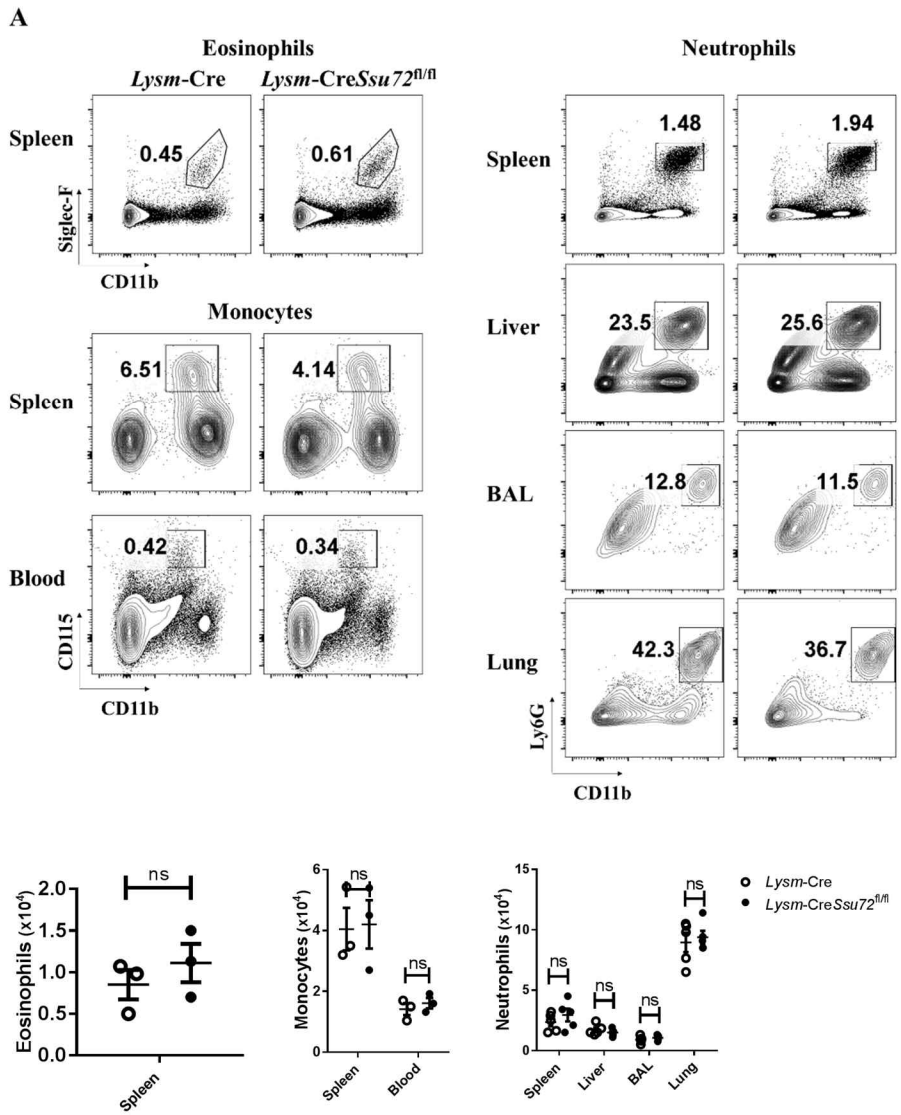
A
Eosinophils
Lysm-Cre
Lysm-CreSsu72fl/fl
Spleen
0.45
0.61
Siglec-F
CD11b
Monocytes
Spleen
6.51
4.14
Blood
0.42
0.34
CD115
CD11b
Neutrophils
Spleen
1.48
1.94
Liver
23.5
25.6
BAL
12.8
11.5
Lung
42.3
36.7
Ly6G
CD11b
Eosinophils (x10⁴)
ns
Spleen
Monocytes (x10⁴)
ns
Spleen
Blood
Neutrophils (x10⁴)
ns
Spleen
Liver
BAL
Lung
Lysm-Cre
Lysm-CreSsu72fl/fl
B
Lysm-Cre
Lysm-CreSsu72fl/fl
ssu72/gapdh
Monocytes
Neutrophils
Eosinophils
C
T cells
Lysm-Cre
Lysm-CreSsu72fl/fl
ssu72/gapdh

Figure 2. Ssu72 is dispensable for development of monocytes, neutrophils and eosinophils

(A) The populations of monocytes, neutrophils, eosinophils were measured in various organs of *Lysm*-Cre and *Lysm*-Cre*Ssu*72$^{fl/fl}$ mice using flow cytometry. Following markers were used for flow cytometric analysis. (Monocytes – CD11b^{+}CD115^{+}, Neutrophils – CD11b^{+}Ly6G^{+} and Eosinophils – CD11b^{+}Siglec-F^{+}). (*n* = 5 per group) (B-C) The expression levels of *ssu72* transcript were measured in (B) monocytes, neutrophils, eosinophils, and (C) T cells (TCRβ^{+}CD19^{-}) sorted from spleens of *Lysm*-Cre and *Lysm*-Cre*Ssu*72$^{fl/fl}$ mice using real-time PCR. Expression levels are represented as a fold change over the expression in cells from *Lysm*-Cre*Ssu*72$^{fl/fl}$ mice. (B; *n* = 10 per group, C; *n* = 3 per group) Data were pooled from five (A), three (B) and 1 (C) independent experiment and presented as means ± SEMS. Ns, Not significant. *P<0.5, **P<0.01, and ***P<0.001

The generation of BMDMs were compared between *Lysm*-Cre and *Lysm*-Cre*Ssu72*$^{fl/fl}$ mice. BMDMs differentiated by M-CSF have been traditionally used as one of the most common method to study macrophages[19]. Successful deletion of Ssu72 in BMDMs from *Lysm*-Cre*Ssu72*$^{fl/fl}$ mice was detected via western blotting. (Figure 3A) The BMDMs generated from *Lysm*-Cre and *Lysm*-Cre*Ssu72*$^{fl/fl}$ mice were similar in their numbers and expression levels of CD11b and F4/80 suggesting that Ssu72 does not play a critical role in generation of BMDMs. (Figure 3B)

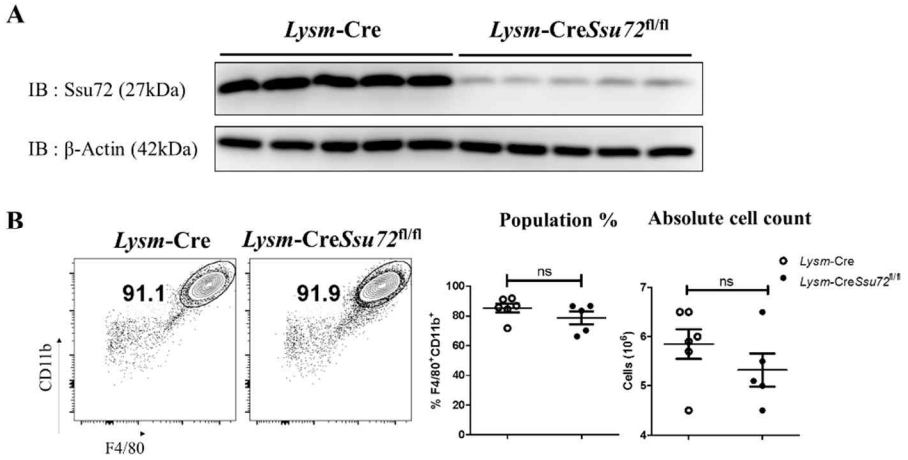

Figure 3. Ssu72 is dispensable for generation of BMDMs.

(A) BMDMs from *Lysm*-Cre and *Lysm*-Cre*Ssu72*$^{fl/fl}$ mice were generated by treatment with M-CSF (20 ng/ml for 6-8 days) and approximately 2.0x10^6 cells were used for each sample of western blotting. (B) Approximately 5.0x10^5 cells were used for flow cytometry analysis of CD11b and F4/80 expression. Only adherent cells were used (A-B). (A; *n* = 10 per group, B; n = 6 per group) Data were pooled from 3 independent experiments and presented as means ± SEMS. Ns, Not significant. *P<0.5, **P<0.01, and ***P<0.001.

Analysis of tissue macrophages in *Lysm*-Cre*Ssu72*$^{fl/fl}$ mice

As mentioned above, recent studies on origins of tissue macrophages suggest the necessity to consider each subset of tissue resident macrophage as a unique entity. Many studies suggest that each tissue resident macrophage subset utilizes unique cytokines and transcriptional factors for their own development and survival. Based on these reports, it seemed reasonable to hypothesize that Ssu72 might regulate development of tissue macrophages.

Tissue macrophages from brains, airways, lungs, livers, spleens, and peritoneum of *Lysm*-Cre and *Lysm*-Cre*Ssu72*$^{fl/fl}$ mice were analyzed via flow cytometry. (Figure 4A) The results showed that while no other macrophage subsets were significantly altered by depleting Ssu72, only lung resident AMs were reduced in their proportion and numbers in absence of Ssu72. In addition, interstitial macrophages (IMs), which is another lung resident macrophage subset showed no changes in proportion or in numbers in absence of Ssu72. (Figure 4A)

One of the possible reasons for this phenomenon is due to different expression levels of *ssu72* in tissue macrophage subsets. To test this, each macrophage subsets were sorted from *Lysm*-Cre and *Lysm*-Cre*Ssu72*$^{fl/fl}$ mice and their *ssu72* expression levels were compared via real-time PCR. Among tissue macrophage subsets, AMs were one of the subsets with the highest *ssu72* expression, but IMs and microglia cells also expressed

ssu72 at the similar level to that of AMs. Tissue macrophage subsets sorted from *Lysm*-Cre*Ssu72*$^{fl/fl}$ mice were all reduced in their *ssu72* expression. (Figure 4B) Put together, these data suggest that although tissue resident macrophages universally express Ssu72, Ssu72 was dispensable for most tissue resident macrophage development but necessary for proper AM development.

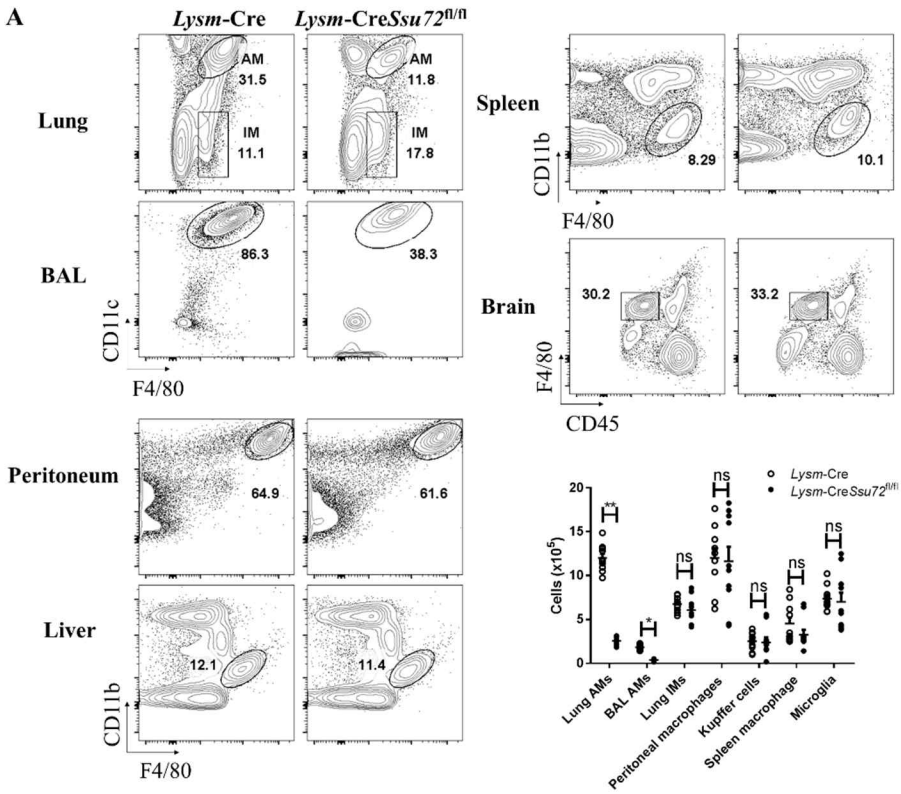
A
Lysm-Cre
Lysm-CreSsu72fl/fl
Lung
AM
31.5
IM
11.1
AM
11.8
IM
17.8
BAL
86.3
38.3
CD11c
F4/80
Spleen
8.29
10.1
CD11b
F4/80
Brain
30.2
33.2
F4/80
CD45
Peritoneum
64.9
61.6
Liver
12.1
11.4
CD11b
F4/80
Cells (x10^5)
Lung AMs
BAL AMs
Lung IMs
Peritoneal macrophages
Kupffer cells
Spleen macrophage
Microglia

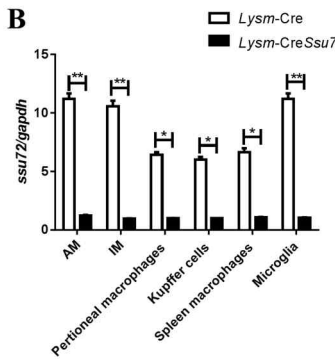
B
Lysm-Cre
Lysm-CreSsu72fl/fl
ssu72/gapdh
AM
IM
Pertioneal macrophages
Kupffer cells
Spleen macrophages
Microglia

Figure 4. Ssu72 regulates development of AMs

(A) Tissue resident macrophages in *Lysm*-Cre and *Lysm*-Cre*Ssu72*$^{fl/fl}$ mice were analyzed via flow cytometry. Following markers were used to identify each subset. Lung AMs – CD45^{+}CD11c^{+}F4/80^{+}, Lung IMs – CD45^{+}CD11c^{-}F4/80^{+}, BAL (broncho-alveolar lavage) AMs – CD45^{+}CD11c^{+}F4/80^{+}, Peritoneal Macrophages – CD45^{+}CD11b^{+}F4/80^{+}, Kupffer cells – CD45^{+}CD11b^{+}F4/80^{+}, Splenic macrophages – CD45^{+}CD11b^{-}F4/80^{+}, Microglia – CD45^{int}CD11b^{+}. Absolute cell numbers were estimated by measuring total number of cells in each tissue and multiplying by percentages of each tissue macrophages. (B) The level of *ssu72* in sorted macrophages from *Lysm*-Cre and *Lysm*-Cre*Ssu72*$^{fl/fl}$ mice were measured via real-time PCR. Expression levels are represented as a fold change over the expression in cells from *Lysm*-Cre*Ssu*72$^{fl/fl}$ mice. (A-B; n = 10 per group) Data were pooled from 3 independent experiments and presented as means ± SEMS. Ns, Not significant. *P<0.5, **P<0.01, and ***P<0.001.

Ssu72 regulates maturation of AMs

The maturation status of AMs can be estimated by measuring surface expression of Siglec-F or CD11b. It is reported that mature AMs highly express Siglec-F while immature AMs express CD11b instead[10]. Using these parameters, the maturation status of AMs in WT and Ssu72-deficient AMs were compared. While WT AMs were mostly mature AMs with high expression of Siglec-F (about 90% of total AMs), Ssu72-absent AMs were lower in Siglec-F expressing mature AMs and higher in CD11b expressing immature AMs than those of WT AMs. (Figure 5A) In accordance with maturational defect detected in Ssu72-deficient AMs, Hematoxylin & Eosin staining of Ssu72-deficient AMs displayed dysregulated granulation and enlarged cytoplasm. (Figure 5B) In addition, some of Ssu72-deficient AMs stained positive with Oil-Red-O staining, indicating that in absence of Ssu72, AMs do not properly process fatty acids. As mentioned briefly in introduction, dysregulation of AMs can result in accumulation of proteins in airway, particularly those of surfactants. Timely surfactant clearance by AMs ensure maximal gas exchange to take place in alveolus[20]. The comparative analysis of total airway protein concentration as well as surfactant D level at different time points of *Lysm*-Cre and *Lysm*-Cre*Ssu72*$^{fl/fl}$ mice revealed overall higher protein concentration as well as surfactant D levels in lungs and airways of *Lysm*-Cre*Ssu72*$^{fl/fl}$ mice than those of

Lysm-Cre mice. (Figure 5C & D) Put together, these findings indicate that a phosphatase Ssu72 regulates the maturation of AMs and timely surfactant clearance in lungs.

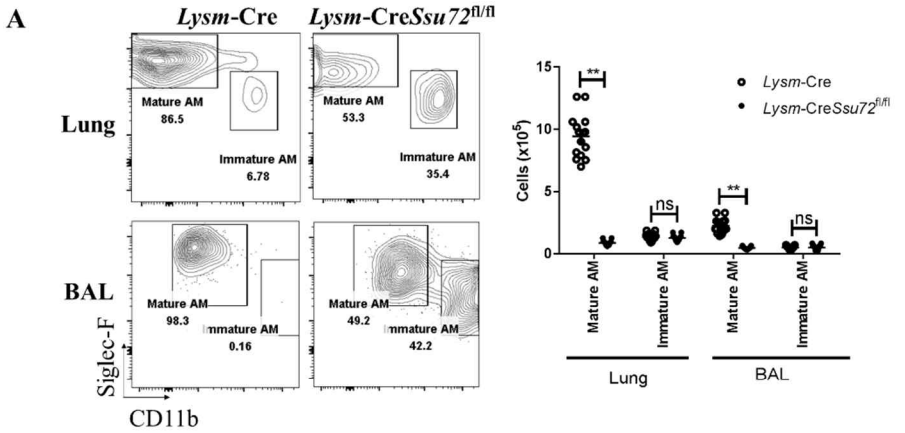
A
Lysm-Cre
Lysm-CreSsu72fl/fl
Lung
BAL
Mature AM
86.5
Immature AM
6.78
Mature AM
53.3
Immature AM
35.4
Mature AM
98.3
Immature AM
0.16
Mature AM
49.2
Immature AM
42.2
Siglec-F
CD11b
Cells (x10^5)
Lysm-Cre
Lysm-CreSsu72fl/fl
Mature AM
Immature AM
Mature AM
Immature AM
Lung
BAL

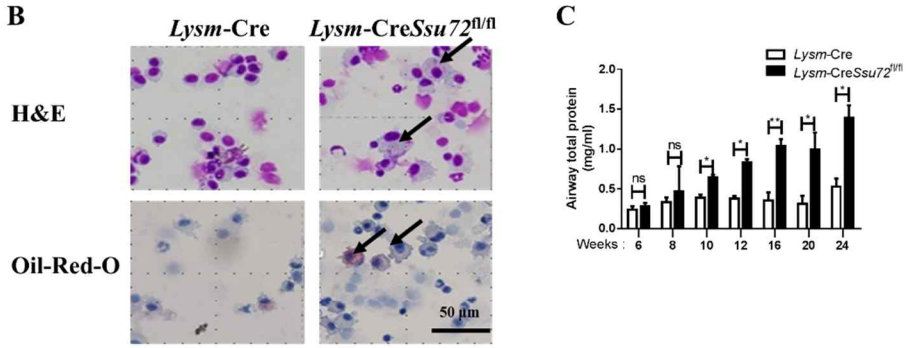
B
Lysm-Cre
Lysm-CreSsu72fl/fl
H&E
Oil-Red-O
50 μm
C
Lysm-Cre
Lysm-CreSsu72fl/fl
Airway total protein (mg/ml)
Weeks : 6 8 10 12 16 20 24

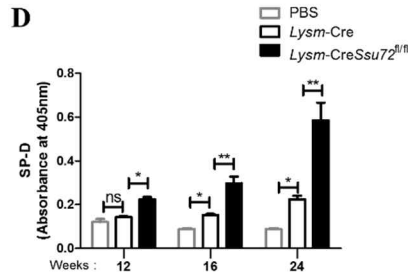
D
PBS
Lysm-Cre
Lysm-CreSsu72fl/fl
SP-D (Absorbance at 405nm)
Weeks : 12 16 24

Figure 5. Ssu72 regulates maturation of AMs.

(A) Maturation status of AMs in lungs and BALs of *Lysm*-Cre and *Lysm*-Cre*Ssu72*$^{fl/fl}$ mice were estimated via flow cytometry. Among F4/80^{+}CD11c^{+} total AMs, Siglec-F^{+}CD11b^{-} cells were considered mature AMs and Siglec-F^{-}CD11b^{+} cells were considered immature AMs. (B) Sorted total AMs from *Lysm*-Cre and *Lysm*-Cre*Ssu72*$^{fl/fl}$ mice were spun down onto microscopic slides using cytospin followed by staining with Hematoxylin and eosin (H&E) stain or Oil-Red-O stain. (C) Total protein concentrations from BAL fluids of *Lysm*-Cre and *Lysm*-Cre*Ssu72*$^{fl/fl}$ mice at indicated weeks were measured for their total protein concentrations using Bradford assay. (D) BAL fluids harvested from *Lysm*-Cre and *Lysm*-Cre*Ssu72*$^{fl/fl}$ mice were measured for surfactant D level using ELISA. Absorbance at 405nm was measured. (A-B; $n = 15$ per group, C-D; $n = 3$ per group) Data were pooled from 5 independent experiments for A-B and 3 independent experiments for C-D and presented as means ± SEMS. Ns, Not significant. *P<0.5, **P<0.01, and ***P<0.001.

Immune cell composition in lungs and BALs of *Lysm*-Cre and *Lysm*-Cre*Ssu72*$^{fl/fl}$ mice

Studies on AMs have suggested that AMs may function as immunosuppressive subset in respiratory system regulating airway tolerance[21]. In addition, AMs have been reported to secrete immune-regulatory factors like Transforming growth factor 1 (TGF-β1) and Interleukin 10 (IL-10) to modulate regulatory T cells (Tregs). Therefore, it is reasonable to assume that there might be changes in immune cell compositions in lungs and BALs of *Lysm*-Cre*Ssu72*$^{fl/fl}$ mice due to dysregulation of AMs. To investigate, immune cell subsets in lungs and BALs of *Lysm*-Cre and *Lysm*-Cre*Ssu72*$^{fl/fl}$ mice were comparatively analyzed via flow cytometry. Flow cytometric analysis revealed similar compositions and numbers of immune cell subsets in lungs and BALs of *Lysm*-Cre and *Lysm*-Cre*Ssu72*$^{fl/fl}$ mice highlighting that reduced proportion and numbers of AMs in *Lysm*-Cre*Ssu72*$^{fl/fl}$ mice had a minimal impact on homeostasis of immune cell subsets within the respiratory tract. (Figure 6)

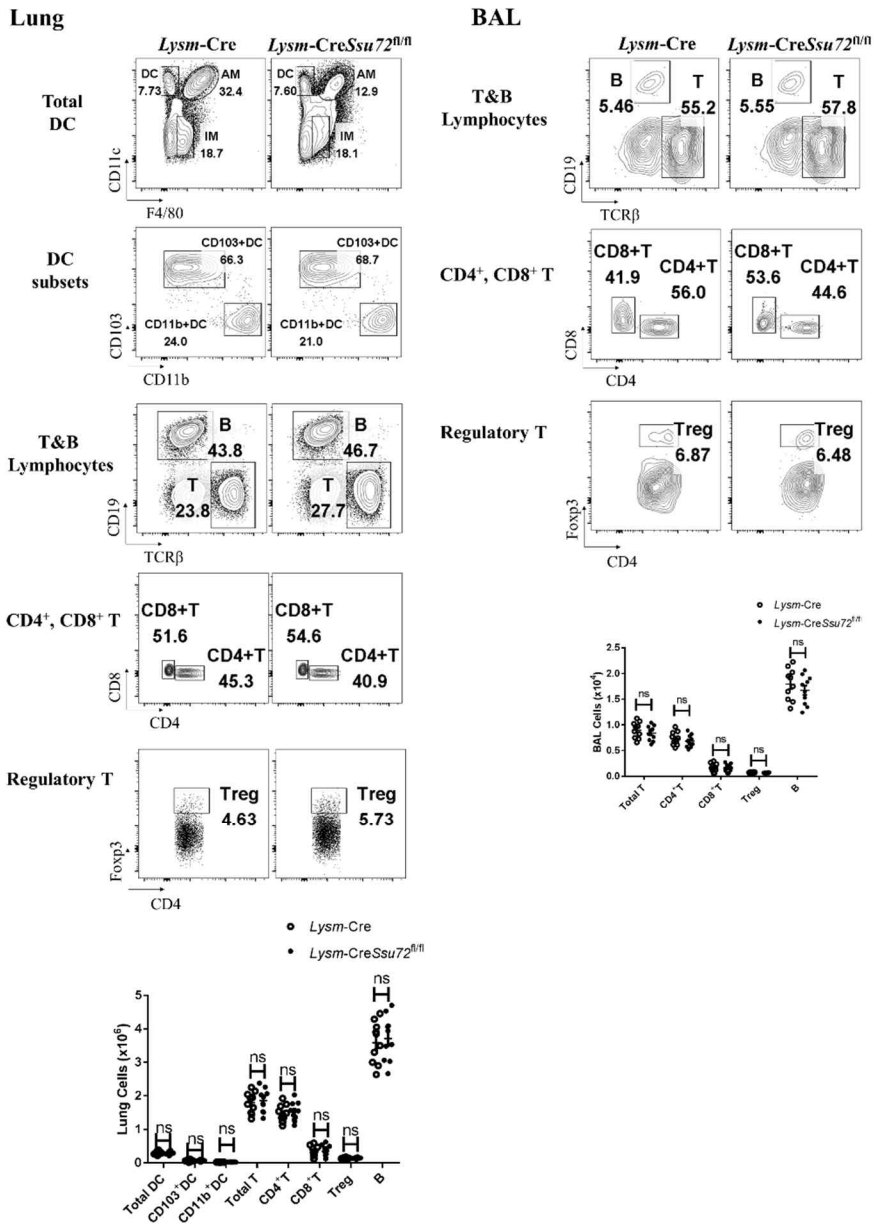
Lung
BAL
Lysm-Cre
Lysm-CreSsu72fl/fl
Total DC
DC
AM
IM
7.73
32.4
18.7
7.60
12.9
18.1
CD11c
F4/80
DC subsets
CD103+DC
66.3
68.7
CD11b+DC
24.0
21.0
CD103
CD11b
T&B Lymphocytes
B
T
43.8
23.8
46.7
27.7
CD19
TCRβ
CD4+, CD8+ T
CD8+T
CD4+T
51.6
45.3
54.6
40.9
CD8
CD4
Regulatory T
Treg
4.63
5.73
Foxp3
5.46
55.2
5.55
57.8
41.9
56.0
53.6
44.6
6.87
6.48
Lung Cells (x10^6)
BAL Cells (x10^4)
ns
Total DC
CD103+DC
CD11b+DC
Total T
CD4+T
CD8+T
Treg
B

Figure 6. Similar immune cell compositions in lungs and BALs between *Lysm*-Cre and *Lysm*-Cre*Ssu72*$^{fl/fl}$ mice.

Immune cell subsets were analyzed in lungs and BALs of *Lysm*-Cre and *Lysm*-Cre*Ssu72*$^{fl/fl}$ mice via flow cytometry. Following markers were used – Total DCs – CD11c^{+}F4/80^{-}, CD103^{+}DCs – CD11c^{+}F4/80^{-}MHC-II^{+}CD103^{+}CD11b^{-}, CD11b^{+}DCs – CD11c^{+}F4/80^{-}MHC-II^{+}CD103^{-}CD11b^{+}, T cells – TCRβ^{+}CD19^{-}, B cells – CD19^{+}TCRβ^{-}, CD4^{+}T cells – TCRβ^{+}CD19^{-}CD4^{+}, CD8^{+}T cells – TCRβ^{+}CD19^{-}CD8^{+}, Tregs – TCRβ^{+}CD19^{-}CD4^{+}Foxp3^{+}. Absolute cell numbers were estimated by measuring total number of cells in each tissue and multiplying by percentages of each immune cell subset. (n = 10 per group) Data were pooled from 3 independent experiments and presented as means ± SEMS. Ns, Not significant. *P<0.5, **P<0.01, and ***P<0.001.

Ssu72 regulates development AMs from neonatal stage.

Fetal monocytes and pre-AMs serve as precursors to AMs which seed lungs at a very early stage and develop into adult mature AMs with minimal contribution from infiltrating monocytes[9]. Primitive hematopoiesis in the yolk sac and definitive hematopoiesis from hematopoietic stem cells contribute differently to the development of tissue macrophages in the embryo[22]. Thus, in order to investigate whether Ssu72 is critical for embryonic and/or fetal development of AMs, *itgax* (gene encoding CD11c; called '*Cd11c'* here)-Cre*Ssu72*$^{fl/fl}$ mice was used instead of *Lysm*-Cre*Ssu*72$^{fl/fl}$ mice because *itgax* expression precedes *lyz2* expression in fetal monocytes. Kinetic analysis revealed that no significant difference was found in generation of fetal monocyte populations at embryonic stages (from E17.5 to E21.1) between *Cd11c*-Cre*Ssu72*$^{fl/fl}$ and *Cd11c*-Cre mice. However, in contrast, the total numbers of pre-AMs were reduced in *Cd11c*-Cre*Ssu72*$^{fl/fl}$ mice at one day after birth, which continued to adulthood. Similarly, analysis of Siglec-F and CD11b expression on AM precursors revealed that AM precursors from *Cd11c*-Cre*Ssu72*$^{fl/fl}$ mice were impaired in maturation to those of *Cd11c*-Cre mice. (Figure 7A) In addition, there was no significant difference in the total number fetal macrophages, which are precursor cells to IMs. (Figure 7A&B) In addition, the expression levels of *ssu72* in different stages of AMs were measured. The expression level

of *ssu72* was higher in pre-AMs than fetal monocytes drawing positive correlation with the kinetic analysis of AM precursors. (Figure 7C) Altogether, these results indicate that Ssu72 regulates the development and maturation of AMs starting at AM precursors, especially during pre-AM stage.

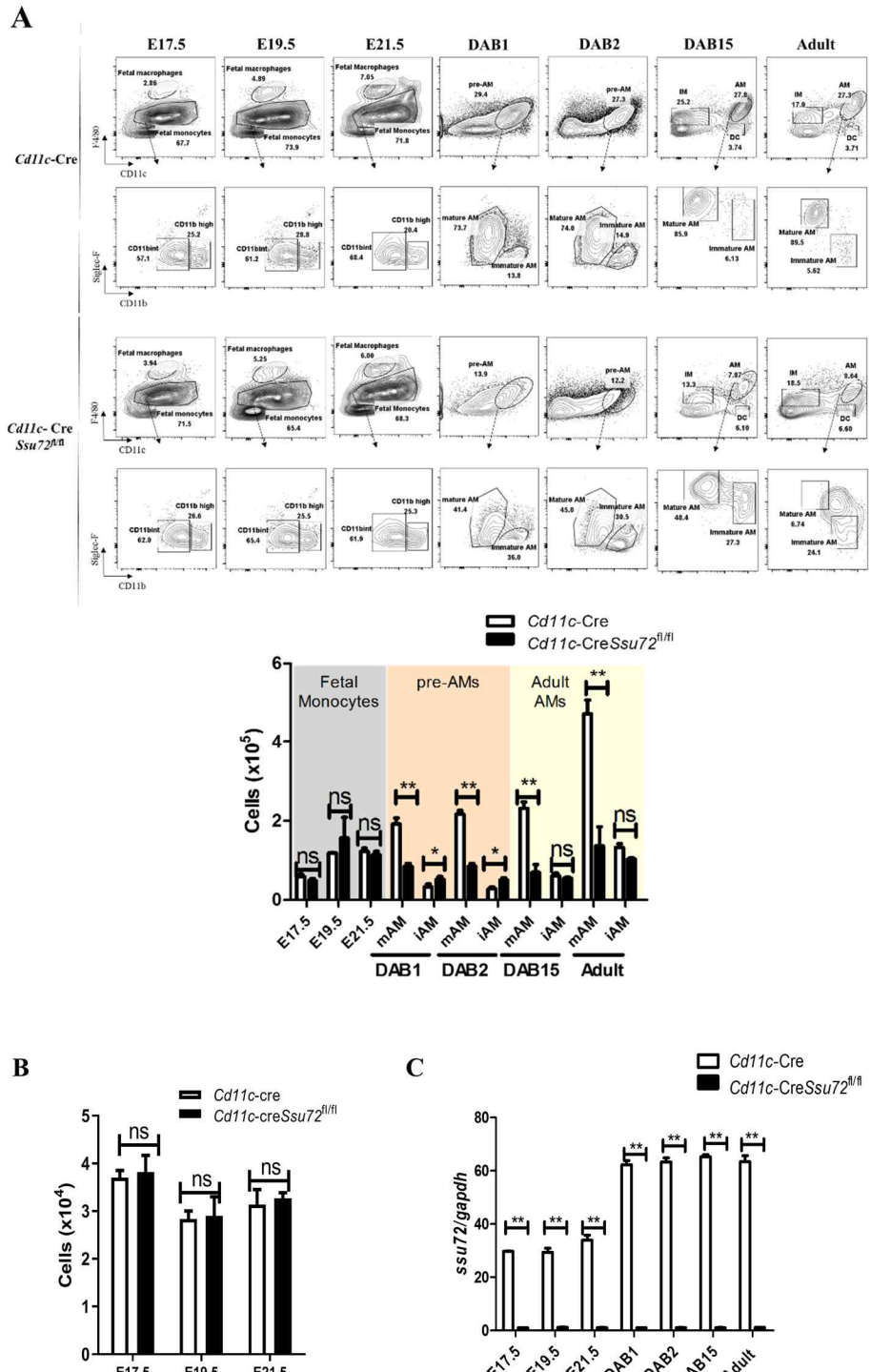
A
E17.5
E19.5
E21.5
DAB1
DAB2
DAB15
Adult
Cd11c-Cre
Cd11c- Cre Ssu72fl/fl
F4/80
CD11c
Siglec-F
CD11b
Fetal macrophages
Fetal monocytes
Fetal Monocytes
pre-AM
IM
AM
DC
CD11b high
CD11bint
mature AM
Mature AM
Immature AM
Cd11c-Cre
Cd11c-CreSsu72fl/fl
Cells (x10^5)
Fetal Monocytes
pre-AMs
Adult AMs
ns
mAM
iAM
B
Cd11c-cre
Cd11c-creSsu72fl/fl
Cells (x10^4)
C
Cd11c-Cre
Cd11c-CreSsu72fl/fl
ssu72/gapdh

Figure 7. Kinetic analysis of AM precursors in *Cd11c*-Cre*Ssu72*$^{fl/fl}$ mice

(A) Lungs of *Cd11c*-Cre*Ssu72*$^{fl/fl}$ and *Cd11c*-Cre mice at indicated time points were harvested and analyzed for fetal monocyte, fetal macrophage, pre-AMs and adult AM populations along with maturation status Absolute cell numbers (A – AM precursors, B – Fetal macrophages) were estimated by multiplying total lung cell numbers to the percentages of desired populations. (C) The level of *ssu72* was measured in sorted AM precursors (fetal monocytes & pre-AMs) from *Cd11c*-Cre*Ssu72*$^{fl/fl}$ and *Cd11c*-Cre mice via real-time PCR. Expression levels are represented as a fold change over the expression in cells from *Cd11c*-Cre*Ssu*72$^{fl/fl}$ mice. (A-B; n = 15 per group, C; n = 8 per group) Data were pooled from 3 independent experiments and presented as means ± SEMS. Ns, Not significant. *P<0.5, **P<0.01, and ***P<0.001.

Ssu72 regulates cellular homeostasis mature AMs

As maturation analysis of AMs have showed, Ssu72 was an important factor regulating numbers of Siglec-F^+ mature AMs, but not that of $CD11b^+$ immature AMs. The expression level of *ssu72* was found higher in already developed mature AMs than that of immature AMs. (Figure 8A) Based on these results, it is reasonable to assume that Ssu72 plays significant roles in already developed Siglec-F^+ mature AMs. To investigate, microarray was conducted to compare transcriptomes of Siglec-F^+ mature AMs from *Lysm*-Cre*Ssu*$72^{fl/fl}$ and *Lysm*-Cre mice. The alteration of gene expressions (108 up-regulated and 600 down-regulated genes) was detected in Ssu72-deficient mature AMs compared to those of WT mature AMs. Down-regulated genes in Ssu72-deficient mature AMs consisted of two categorized groups: genes related to cellular homeostasis (apoptosis, cell cycle, and cell differentiation) and functions (immune response and response to stress). (Figure 8B) To examine the role of Ssu72 in cellular homeostasis of mature AMs, apoptosis and cell cycle of mature AMs were measured first. Ssu72-deficient mature AMs exhibited more apoptotic cells as well as necrotic cells compared to those of WT mature AMs. (Figure 8C) Consistent with this data, Ssu72-deficient mature AMs showed higher expression of pro-apoptotic genes such as *bak1*, *bax*, *puma* and *bim*, but showed lower expression of anti-apoptotic genes like *bcl2* and *bcl-xl* than those of WT mature AMs.

(Figure 8D) Direct DNA staining results showed that Ssu72-deficient mature AMs were arrested at G0 and G1 phases, whereas WT mature AMs were mostly at G2 or M phases. No difference in cell cycle status was found between IMs from two mice group. (Figure 8E) In accordance with cell cycle analysis, Ssu72 deficient mature AMs displayed higher *ccnd1* expression (which encodes Cyclin D) and lower *ccna2* (which encodes Cyclin A) than those of WT mature AMs while expression levels of cyclins in Ssu72-deficient IMs were similar to those of WT IMs. (Figure 8F) It is reported that increase in Cyclin D expression is commonly found in cells in G0 or G1 phase of cell cycle and that decrease in Cyclin D and increase in Cyclin A expression is critical for cells to enter S phase[23]. Therefore, high expression of *ccnd1* and low expression of *ccna2* in Ssu72-deficient mature AMs further suggests that these cells are arrested at G0 & G1 phase of cell cycle. Put together, microarray analysis of WT mature AMs and Ssu72-deficient mature AMs as well as measurement of cell death and cell cycle status in mature AMs show that Ssu72 regulates cellular homeostasis of mature AMs.

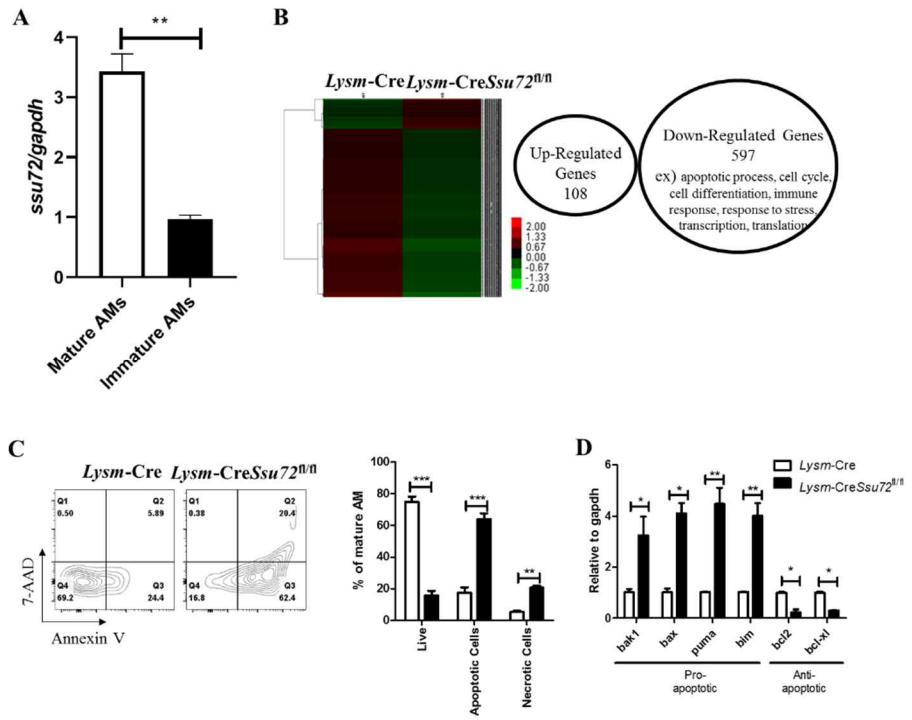

Figure 8. Ssu72 regulates cellular homeostasis of mature AMs

(A) Expression level of *ssu72* was measured in mature AMs and immature AMs sorted from lungs of naïve C57BL/6 wild-type (WT) mice via real-time PCR. Expression levels are represented as a fold change over the expression in cells from immature AMs. (n = 5 per group) (B) Sorted mature AMs from *Lysm*-Cre*Ssu*72$^{fl/fl}$ and *Lysm*-Cre mice were analyzed by microarray analysis. (n = 8 per group) (C) Cell death of mature AMs was measured by staining with Annexin V and 7-AAD in room temperature for 15 mins. Annexin V single positive cells were named as apoptotic cells and Annexin V and 7-AAD double positive cells were named necrotic cells. (n = 12 per group) (D) Sorted mature AMs from *Lysm*-Cre*Ssu*72$^{fl/fl}$ and *Lysm*-Cre mice were analyzed for their pro-apoptotic and anti-apoptotic gene expressions via real-time PCR. (n = 12 per group) Expression levels are represented as a fold change over the expression in cells from mature AMs of *Lysm*-Cre mice.

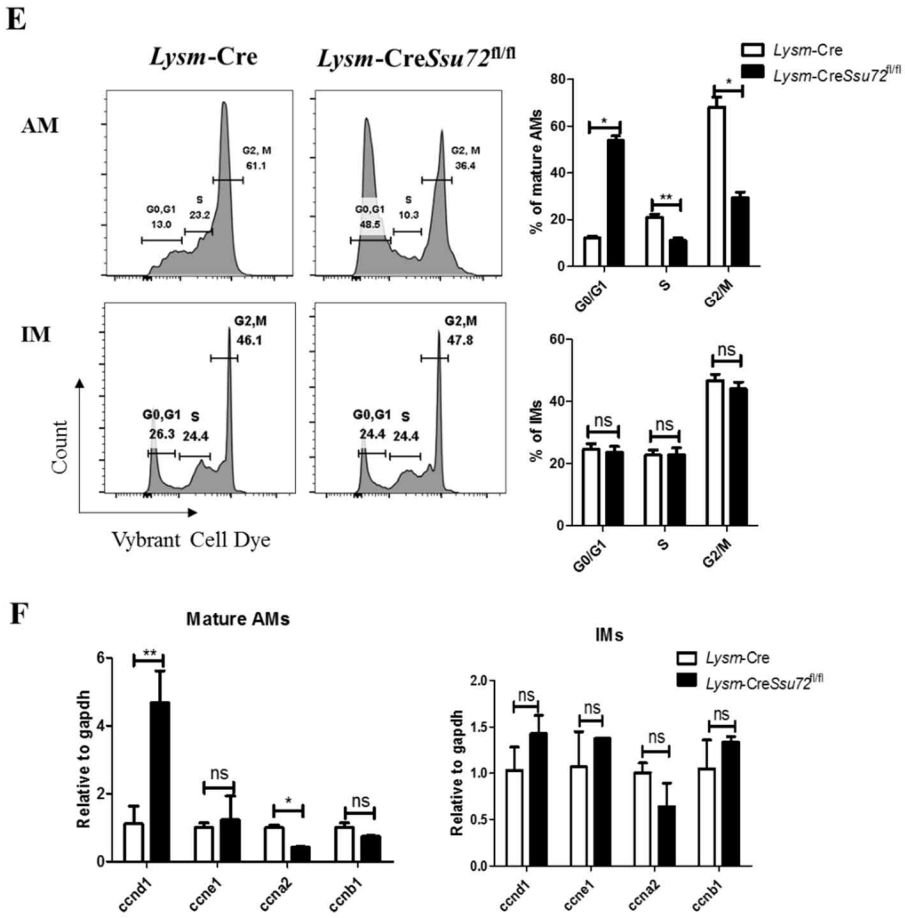

Figure 8. Ssu72 regulates cellular homeostasis of mature AMs (Continued)

(E) Sorted mature AMs and IMs from *Lysm*-Cre*Ssu*72$^{fl/fl}$ and *Lysm*-Cre mice were stained with vybrant cell dye at room temperature for 1 hr followed by washing with 1× PBS twice. (F) Sorted mature AMs and IMs from *Lysm*-Cre*Ssu*72$^{fl/fl}$ and *Lysm*-Cre mice were analyzed for their cyclin expressions via real-time PCR. Expression levels are represented as a fold change over the expression in cells from *Lysm*-Cre*Ssu*72$^{fl/fl}$ mice. (E-F; n = 15 per group) Data were pooled from 5 independent experiments and presented as means ± SEMS. Ns, Not significant. *P<0.5, **P<0.01, and ***P<0.001.

Ssu72 regulates functionalities of mature AMs

Microarray analysis of mature AMs also revealed that Ssu72 deficient mature AMs were defective in their immune responses as well. AMs are one of the first immune cells to encounter antigens in respiratory tract. AMs express variety of pattern recognition receptors like mannose receptor, Toll-like receptors (TLRs), the scavenger receptors, etc[24]. Therefore, it is important for AMs to properly uptake antigens to ensure proper immune response to follow. Antigen uptake capacity in WT mature AMs and Ssu72-deficient mature AMs were measured with treatment with FITC-tagged ovalbumin (OVA) antigen. Compared to the antigen uptake capacity of WT mature AMs, Ssu72-deficient mature AMs were impaired in antigen uptake capacity. (Figure 9A) In addition to antigen uptake capacity, Ssu72-deficient mature AMs were also impaired in their response to TLR4 stimulus. While LPS treatment induced high expression of TNF-α, MHC-I and MHC-II expression in WT mature AMs, Ssu72-deficient mature AMs could not. (Figure9B & C) Altogether, these data suggest that Ssu72-deficient mature AMs are defective in their immunological functions.

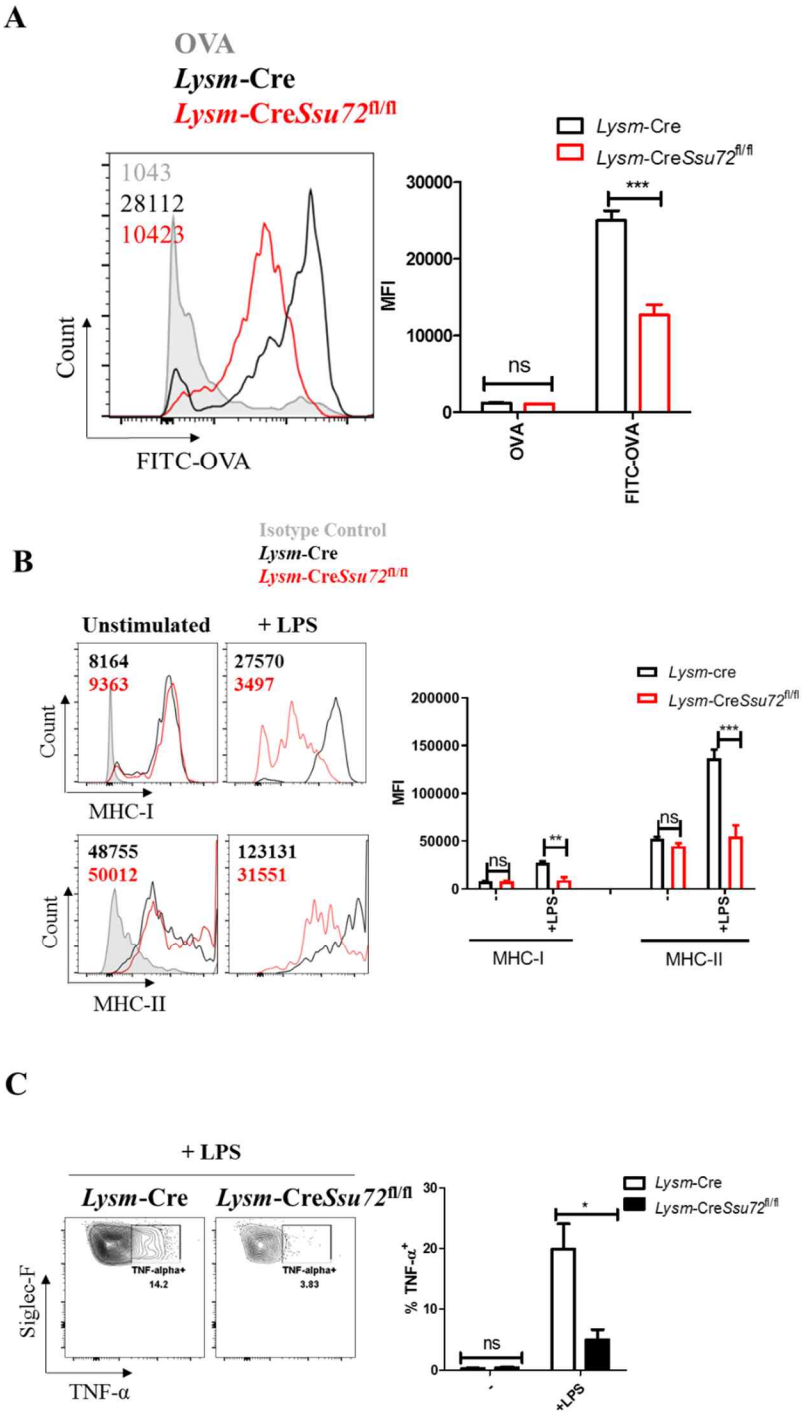
A
OVA
Lysm-Cre
Lysm-CreSsu72fl/fl
1043
28112
10423
Count
FITC-OVA
Lysm-Cre
Lysm-CreSsu72fl/fl
MFI
30000
20000
10000
0
***
ns
OVA
FITC-OVA
B
Isotype Control
Lysm-Cre
Lysm-CreSsu72fl/fl
Unstimulated
+ LPS
8164
9363
27570
3497
Count
MHC-I
48755
50012
123131
31551
Count
MHC-II
Lysm-cre
Lysm-CreSsu72fl/fl
MFI
200000
150000
100000
50000
0
ns
**
ns
***
-
+LPS
-
+LPS
MHC-I
MHC-II
C
+ LPS
Lysm-Cre
Lysm-CreSsu72fl/fl
TNF-alpha+
14.2
TNF-alpha+
3.83
Siglec-F
TNF-α
Lysm-Cre
Lysm-CreSsu72fl/fl
% TNF-α+
30
20
10
0
*
ns
-
+LPS

Figure 9. Ssu72 regulates functionalities of mature AMs

(A) Antigen uptake capacity was measured in sorted mature AMs from *Lysm*-Cre*Ssu*72$^{fl/fl}$ and *Lysm*-Cre mice via flow cytometry. Mature AMs were treated with regular ovalbumin (OVA) antigen or FITC-tagged OVA antigen for 4 h at 37˚C. Samples treated with regular OVA antigen were used as a negative control to the experiment. (B&C) Sorted mature AMs from *Lysm*-Cre*Ssu*72$^{fl/fl}$ and *Lysm*-Cre mice were sorted via flow cytometry. Mature AMs were treated with either 1× PBS (unstimulated group) or LPS (100 ng/ml) for 4 h and analyzed for their MHC-I, II and TNF-α expressions. (A-C; n = 12 per group) Data were pooled from 4 independent experiments and presented as means ± SEMS. Ns, Not significant. *P<0.5, **P<0.01, and ***P<0.001.

Ssu72 regulates mitochondrial respiration of mature AMs

In addition to whole transcriptome analysis of microarray data, Kyoto Encyclopedia of Genes and Genomes (KEGG) pathway analysis of microarray data revealed that the expression levels of genes related to oxidative phosphorylation were decreased in Ssu72-deficient mature AMs compared with those of WT mature AMs. (Figure 10A) Consistently, oxygen consumption rate (OCR) was also reduced in Ssu72-deficient mature AMs to that of WT mature AMs, whereas extracellular acidification rate (ECAR) was similar between the two. (Figure 10B) Furthermore, Ssu72-deficient mature AMs showed enhancement in mitochondria reactive oxygen species (ROS) levels, and membrane potential but reduction in mitochondrial mass at different time points of development than those of WT mature AMs. Starting from 1 day after birth, Ssu72-deficient mature AMs already showed significant reduction in mitochondrial mass to that of WT mature AMs. Mitochondrial ROS is a direct result of electron leakage at complex I and complex III from electron transport chains. Therefore, the level of mitochondrial ROS can be used as a hallmark for assessing the capacity of oxidative phosphorylation[25]. In addition, there are reports that suggest high levels of mitochondrial ROS can directly activate apoptosis and autophagy pathways to induce cell death highlighting the importance of mitochondrial homeostasis in overall cell survival[26]. The calculation of

mitochondria ROS level per mass of mitochondria revealed much higher mitochondria ROS level in Ssu72-deficient mature AMs than that of WT mature AMs suggesting improper oxidative phosphorylation in Ssu72-deficient mature AMs. (Figure 10C) Though not directly tested here, increase in relative mitochondrial ROS level might also explain increased apoptosis and necrosis detected in Ssu72-deficient mature AMs to those of WT mature AMs. The expression levels of major transcription factors responsible for mitochondrial functions including *yy1, ulk1* and *vdac1* were reduced in Ssu72-deficient mature AMs. However, the genes related to mitochondrial biogenesis or electron transport chain (ETC) were increased in Ssu72-deficient mature AMs, suggesting that compensatory enhancement of mitochondrial biogenesis and ETC might be occurring in these cells. (Figure 10D). Taken together, these results show that Ssu72-deficient mature AMs are defective in their oxidative phosphorylation capacity and that this may be one of the key factors contributing to cause improper cellular homeostasis detected in Ssu72-deficient mature AMs.

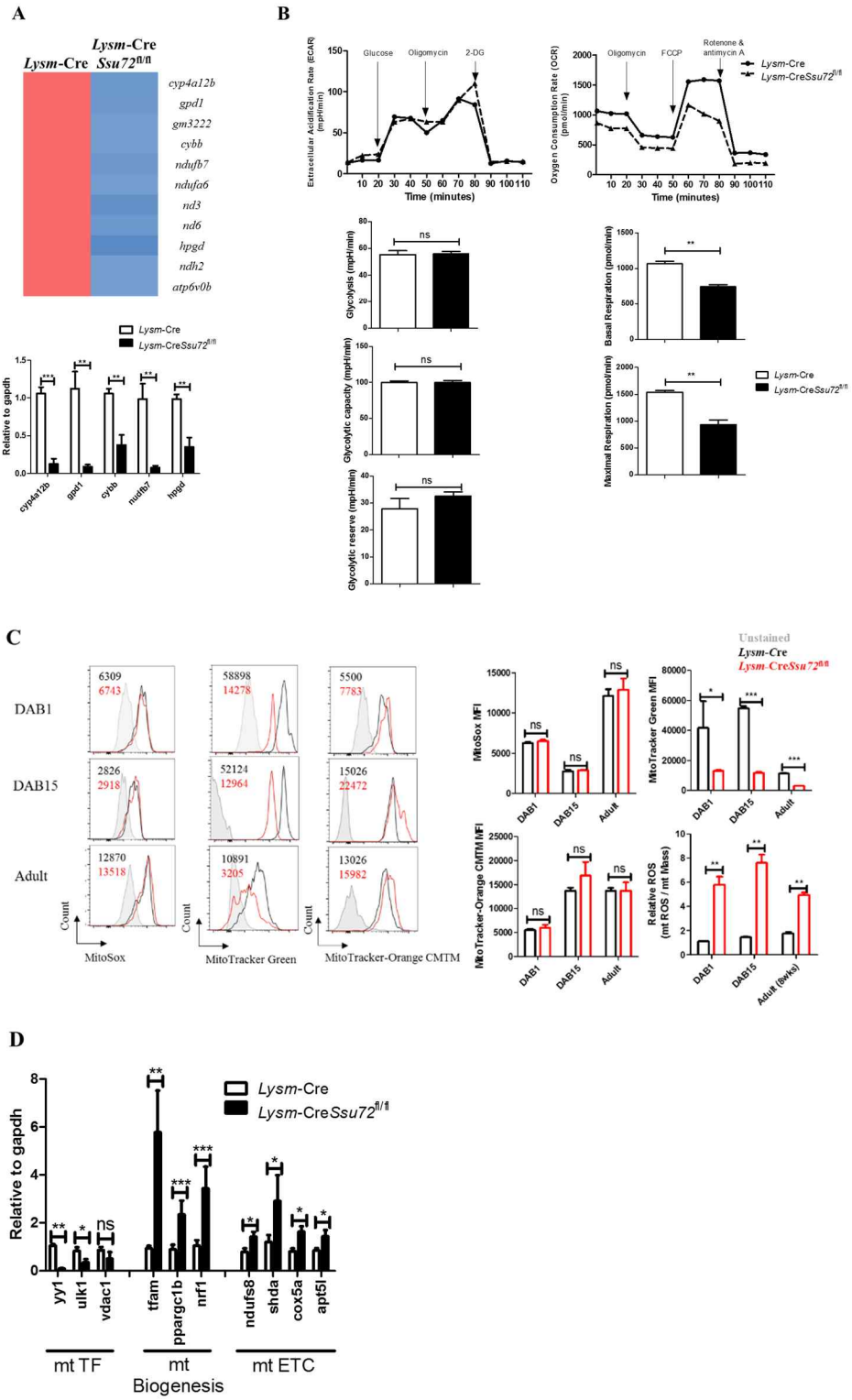
A
Lysm-Cre
Lysm-Cre Ssu72fl/fl
cyp4a12b
gpd1
gm3222
cybb
ndufb7
ndufa6
nd3
nd6
hpgd
ndh2
atp6v0b
Lysm-Cre
Lysm-CreSsu72fl/fl
Relative to gapdh
cyp4a12b
gpd1
cybb
ndufb7
hpgd
B
Extracellular Acidification Rate (ECAR) (mpH/min)
Glucose
Oligomycin
2-DG
Time (minutes)
Oxygen Consumption Rate (OCR) (pmol/min)
Oligomycin
FCCP
Rotenone & antimycin A
Lysm-Cre
Lysm-CreSsu72fl/fl
Time (minutes)
Glycolysis (mpH/min)
Glycolytic capacity (mpH/min)
Glycolytic reserve (mpH/min)
ns
Basal Respiration (pmol/min)
Maximal Respiration (pmol/min)
**
Lysm-Cre
Lysm-CreSsu72fl/fl
C
Unstained
Lysm-Cre
Lysm-CreSsu72fl/fl
DAB1
DAB15
Adult
6309
6743
58898
14278
5500
7783
2826
2918
52124
12964
15026
22472
12870
13518
10891
3205
13026
15982
Count
MitoSox
MitoTracker Green
MitoTracker-Orange CMTM
MitoSox MFI
MitoTracker Green MFI
MitoTracker-Orange CMTM MFI
Relative ROS (mt ROS / mt Mass)
DAB1
DAB15
Adult
Adult (8wks)
D
Lysm-Cre
Lysm-CreSsu72fl/fl
Relative to gapdh
yy1
ulk1
vdac1
tfam
ppargc1b
nrf1
ndufs8
shda
cox5a
apt5l
mt TF
mt Biogenesis
mt ETC

Figure 10. Ssu72 regulates mitochondrial respiration of mature AMs

(A) KEGG pathway analysis of microarray analysis of mature AMs from *Lysm*-Cre*Ssu*72$^{fl/fl}$ and *Lysm*-Cre mice. Mature AMs from *Lysm*-Cre*Ssu*72$^{fl/fl}$ and *Lysm*-Cre mice were sorted and measured for some of the suggested genes in the pathway analysis via real-time PCR. Expression levels are represented as a fold change over the expression in cells from *Lysm*-Cre mice (B) Sorted mature AMs from *Lysm*-Cre*Ssu*72$^{fl/fl}$ and *Lysm*-Cre mice were seeded at XF24 cell culture microplates at 2.0x10^5 per well to analyze ECAR and OCR. (C) Sorted AM precursors or mature AMs at indicated birth periods from *Lysm*-Cre*Ssu*72$^{fl/fl}$ and *Lysm*-Cre mice were treated with the following reagents - MitoSox 1μM, MitoTracker Green 100nM, MitoTracker-Orange CMTM 100nM to measure for their mitochondrial ROS, mass and membrane potential respectively. (D) Expression levels of transcripts of mitochondria transcription factors, biogenesis and electron transport chain (ETC) related were measured in mature AMs sorted from *Lysm*-Cre*Ssu*72$^{fl/fl}$ and *Lysm*-Cre mice via real-time PCR. Expression levels are represented as a fold change over the expression in cells from *Lysm*-Cre*Ssu*72$^{fl/fl}$ mice. (A-D; n = 14 per group) Data were pooled from 4 independent experiments and presented as means ± SEMS. Ns, Not significant. *P<0.5, **P<0.01, and ***P<0.001.

Ssu72 regulates GM-CSF signaling in AMs via binding to GM-CSFR βc

GM-CSF has been reported to play a critical role in the development and maturation of AMs, but not that of other tissue resident macrophages. GM-CSFR mainly consists of two chains – α-chain (CD116) which is directly responsible for binding to GM-CSF and β-chain (CD131), which is a signal transducing chain also utilized by Interleukin 3 (IL-3) and Interleukin 5 (IL-5) as well[27]. In addition, it has been reported that GM-CSF signaling functions like a binary switch in that amount of GM-CSF treated brings about different cellular outcomes. While small amount of GM-CSF treatment results in phosphorylation of serine residues of GM-CSFR βc which leads to survival of cells, large amount of GM-CSF treatment results in phosphorylation of tyrosine residues of GM-CSFR βc which leads to survival and proliferation of cells. Based on these reports, it is reasonable to hypothesize that Ssu72 phosphatase might regulate GM-CSF signaling by regulating phosphorylation of GM-CSFR βc. To investigate, the amount of GM-CSF in the lungs of *Lysm*-Cre*Ssu72*$^{fl/fl}$ mice to that of *Lysm*-Cre mice and expression levels of GM-CSF receptor α or β chain on mature AMs were measured and found comparable between the two groups. (Figure 11 A&B) This result led to hypothesize that Ssu72 might directly affect GM-CSFR signaling cascade in AMs by dephosphorylating downstream proteins.

Consistently, GM-CSF treatment increased, peaked, and rapidly decreased the level of *ssu72* expression in WT mature AMs in a dose dependent manner, whereas M-CSF treatment did not. (Figure 11 C&D) Moreover, upon GM-CSF treatment, Ssu72-deficient BMDMs displayed higher levels of phosphorylation both at tyrosine and serine residues of GM-CSFR βc and subsequent GM-CSF signaling cascade proteins such as JAK2, STAT5, ERK1/2 than those of WT BMDMs. (Figure 11E&F) In addition, cytosolic/nuclear fraction and confocal microscopy on BMDMs and AMs showed that Ssu72 was dominantly expressed in cytosols of mature AMs instead of nucleus, even though Ssu72 has been reported to act as a phosphatase binding with CTD domains of RNAP-II in the nucleus. (Figure 12A&B) Thus, these findings altogether suggest that Ssu72 might directly bind to and dephosphorylate GM-CSFR βc. Consistent with this hypothesis, co-immunoprecipitation assay showed that Ssu72 and GM-CSFR βc in BMDMs directly bound to each other upon treatment with GM-CSF, which was consistently found in AMs, but not in IMs. (Figure 12C&D) Lastly, the expression levels of *pparg* was lower in Ssu72-deficient mature AMs than that of WT mature AMs suggesting that stronger GM-CSF signaling is not favorable for mature AMs. (Figure12E) Combined, these results indicate that Ssu72 inhibits phosphorylation of GM-CSFR βc and its downstream signaling proteins via binding to GM-CSFR βc.

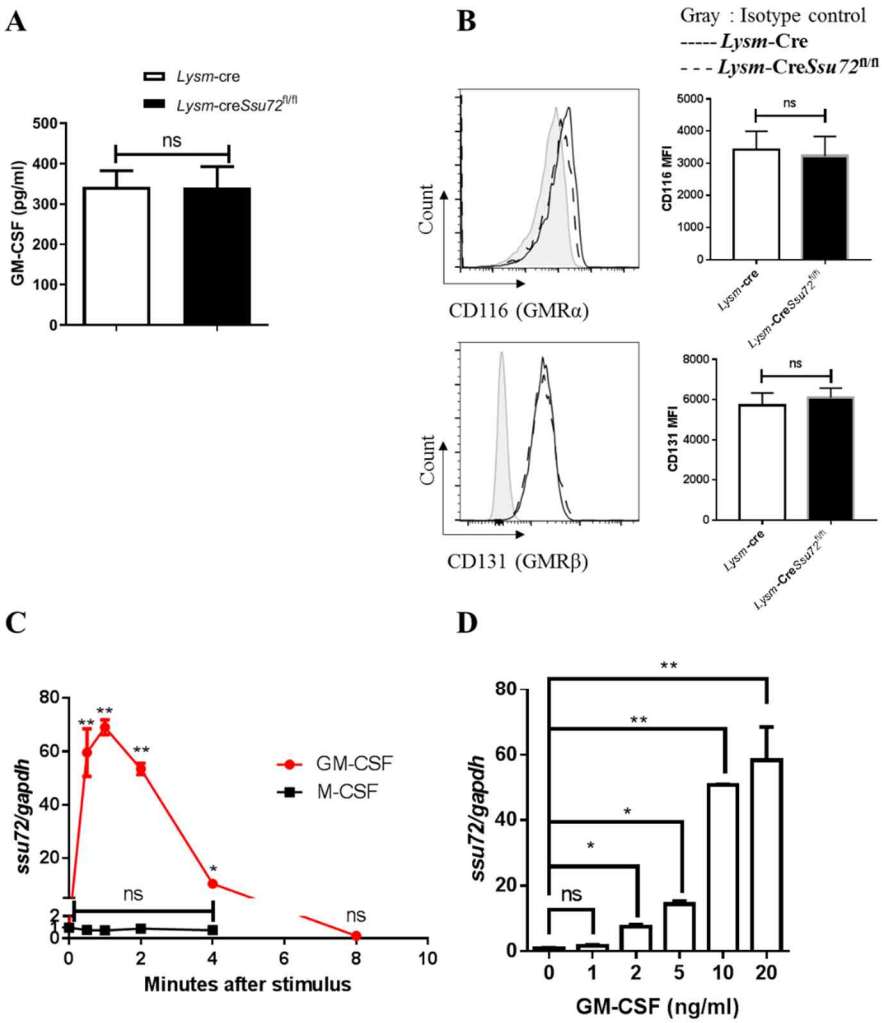
A
Lysm-cre
Lysm-creSsu72fl/fl
GM-CSF (pg/ml)
ns
B
Gray : Isotype control
----- Lysm-Cre
- - - Lysm-CreSsu72fl/fl
Count
CD116 (GMRα)
CD116 MFI
ns
Lysm-cre
Lysm-CreSsu72fl/fl
Count
CD131 (GMRβ)
CD131 MFI
ns
C
ssu72/gapdh
GM-CSF
M-CSF
ns
Minutes after stimulus
D
ssu72/gapdh
GM-CSF (ng/ml)

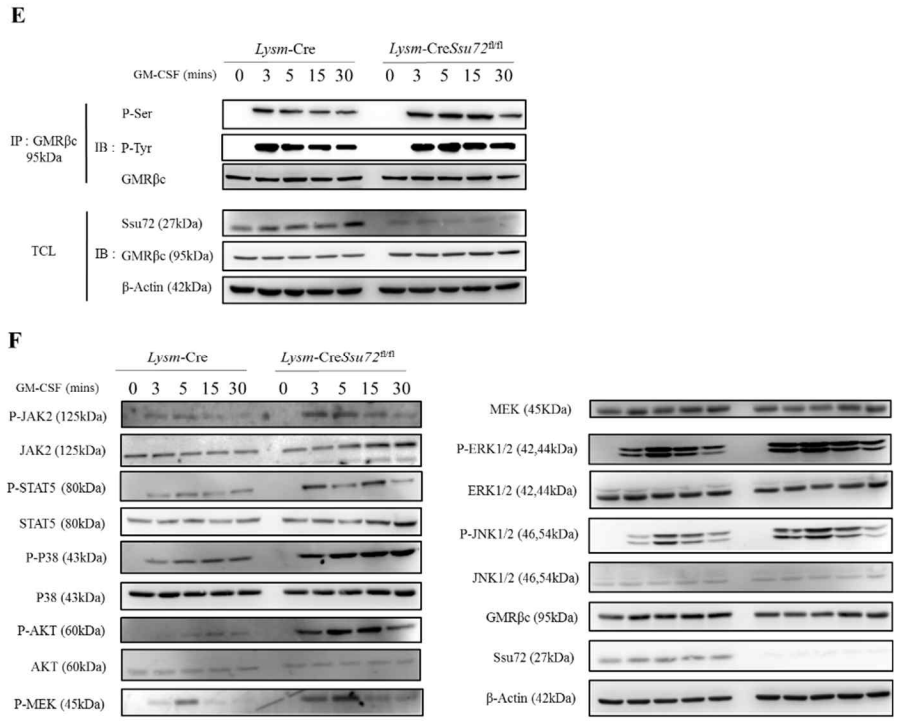

Figure 11. Phosphatase Ssu72 regulates phosphorylation of GM-CSFR signaling

(A) Total lung GM-CSF levels from *Lysm*-Cre*Ssu*72$^{fl/fl}$ and *Lysm*-Cre mice were measured via enzyme linked immunosorbent assay (ELISA). The lungs were homogenized in 1 mL of 1× PBS and supernatants were used for ELISA. (B) Expression levels of CD116 and CD131 were measured in mature AMs from *Lysm*-Cre*Ssu*72$^{fl/fl}$ and *Lysm*-Cre mice (C) WT mature AMs were sorted and treated with GM-CSF (20 ng/ml) or M-CSF (20 ng/ml) and *ssu72* expression was measured via real-time PCR. (D) Sorted WT mature AMs were treated with increasing doses of GM-CSF for 1 min and *ssu72* expression was estimated via real-time PCR. (A-B; n = 8 per group, C-D; n = 6 per group) Expression levels are represented as a fold change over the expression in cells before treatment with GM-CSF or M-CSF (0 mins). (E-F) BMDMs from *Lysm*-Cre*Ssu*72$^{fl/fl}$ and *Lysm*-Cre were stimulated with GM-CSF (20 ng/ml) for

indicated time points. Approximately $2.0x10^6$ cells were used for each sample. (E) BMDMs were immunoprecipitated with anti-GM-CSFR βc antibody followed by treatment with agarose beads overnight before proceeding to western blot. (F) Phosphorylation of GM-CSF downstream proteins as well as amount of total proteins were measured with indicated antibodies. (*n* = 14 per group) Data were pooled from 5 independent experiments and presented as means ± SEMS. Ns, Not significant. *P<0.5, **P<0.01, and ***P<0.001.

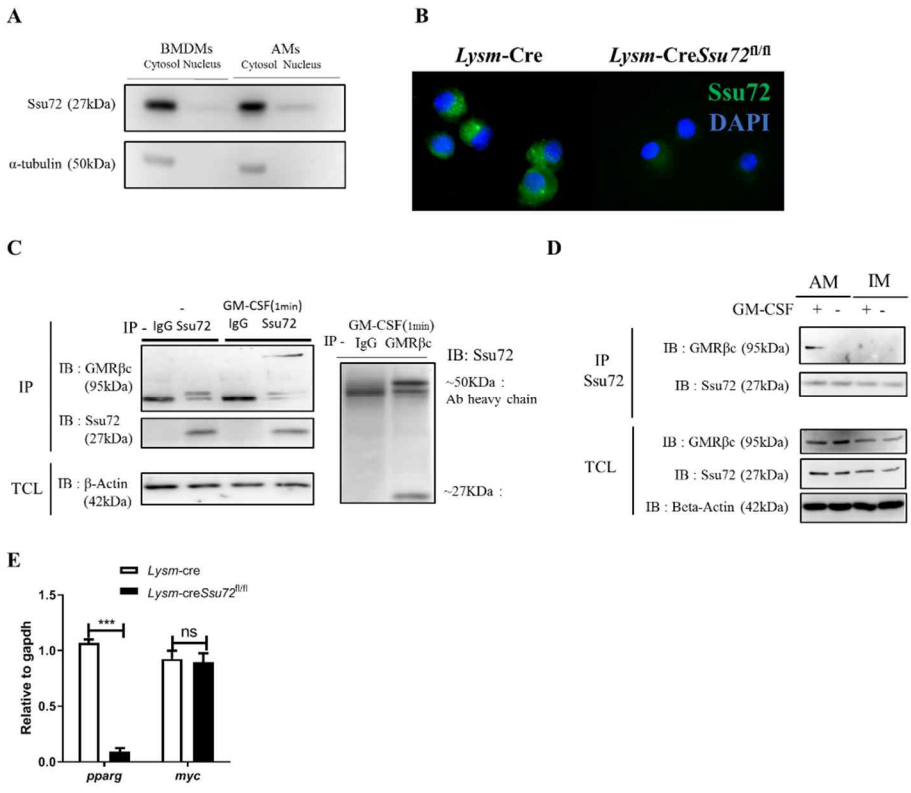
A
BMDMs
AMs
Cytosol Nucleus
Cytosol Nucleus
Ssu72 (27kDa)
α-tubulin (50kDa)
B
Lysm-Cre
Lysm-CreSsu72fl/fl
Ssu72
DAPI
C
IP
TCL
IB : GMRβc (95kDa)
IB : Ssu72 (27kDa)
IB : β-Actin (42kDa)
IP - IgG Ssu72
GM-CSF(1min)
IgG Ssu72
IP - IgG GMRβc
GM-CSF(1min)
IB: Ssu72
~50KDa : Ab heavy chain
~27KDa :
D
AM
IM
GM-CSF + - + -
IP Ssu72
IB : GMRβc (95kDa)
IB : Ssu72 (27kDa)
TCL
IB : GMRβc (95kDa)
IB : Ssu72 (27kDa)
IB : Beta-Actin (42kDa)
E
Lysm-cre
Lysm-creSsu72fl/fl
Relative to gapdh
1.5
1.0
0.5
0.0
***
ns
pparg
myc

Figure 12. Ssu72 directly binds to GM-CSFR βc

(A) WT BMDMs and sorted WT mature AMs' cytosols and nucleus were separated and Ssu72 expressions were measured via western blotting. (B) Sorted mature from AMs *Lysm*-Cre*Ssu*72$^{fl/fl}$ and *Lysm*-Cre were centrifuged onto microscopic slides by cytospin method. The slides were first stained with DAPI staining for 1 hr at room temperature (RT) followed by staining with anti-Ssu72 antibody for 1 hr at RT and visualized under confocal microscope. (C) WT BMDMs were stimulated with GM-CSF (20 ng/ml) for 1 min and cells were incubated with either anti-IgG or anti-Ssu72 or anti-GM-CSFR βc antibodies. (D) WT mature AMs and IMs were sorted and stimulated with GM-CSF (20 ng/ml) for one minute. Cells were incubated with either anti-IgG or anti-Ssu72 antibodies. (E) Expression level of *pparg* and *myc* were measured in sorted mature AMs from *Lysm*-Cre*Ssu*72$^{fl/fl}$ and *Lysm*-Cre via real-time PCR. Expression levels are represented as a fold change over the expression in cells from *Lysm*-Cre*Ssu*72$^{fl/fl}$ mice. (A-B; n = 8 per group, C-D; n = 10 per group, E; n = 6 per group) Data were pooled from 4 independent experiments and presented as means ± SEMS. Ns, Not significant. *P<0.5, **P<0.01, and ***P<0.001.

Ssu72 regulates lung CD103^{+}DCs.

Since Ssu72 directly regulates GM-CSF signaling in AMs, it seemed reasonable to question whether Ssu72 regulates other immune cells dependent upon GM-CSF. CD103^{+}DCs, one of the common subsets of conventional dendritic cells (cDCs) is known to depend upon GM-CSF for its development[28]. In order to test this hypothesis, CD103^{+}DCs in lungs and its analogous subset of CD8α^{+} DCS in spleens were analyzed in *Cd11c*-Cre*Ssu72*$^{fl/fl}$ and in *Cd11c*-Cre mice. While lung CD103^{+}DCs numbers were significantly reduced in *Cd11c*-cre*Ssu72*$^{fl/fl}$ than that of Cd11c-cre mice, no significant changes were detected in splenic CD8α^{+}DCs. (Figure 13A) The tissue restricted changes might be due to differential expression of GM-CSF in various tissues. Analysis of GM-CSF levels in various tissues revealed that while lungs contain relatively high levels of GM-CSF, spleens were low in their GM-CSF level. (Figure 13B) This might explain the changes in lung CD103^{+}DCs of *Cd11c*-Cre*Ssu72*$^{fl/fl}$ mice but not in splenic CD8α^{+} DCs but further investigation is required to conclusively determine the mechanism behind Ssu72 mediated regulation of lung CD103^{+}DCs.

A

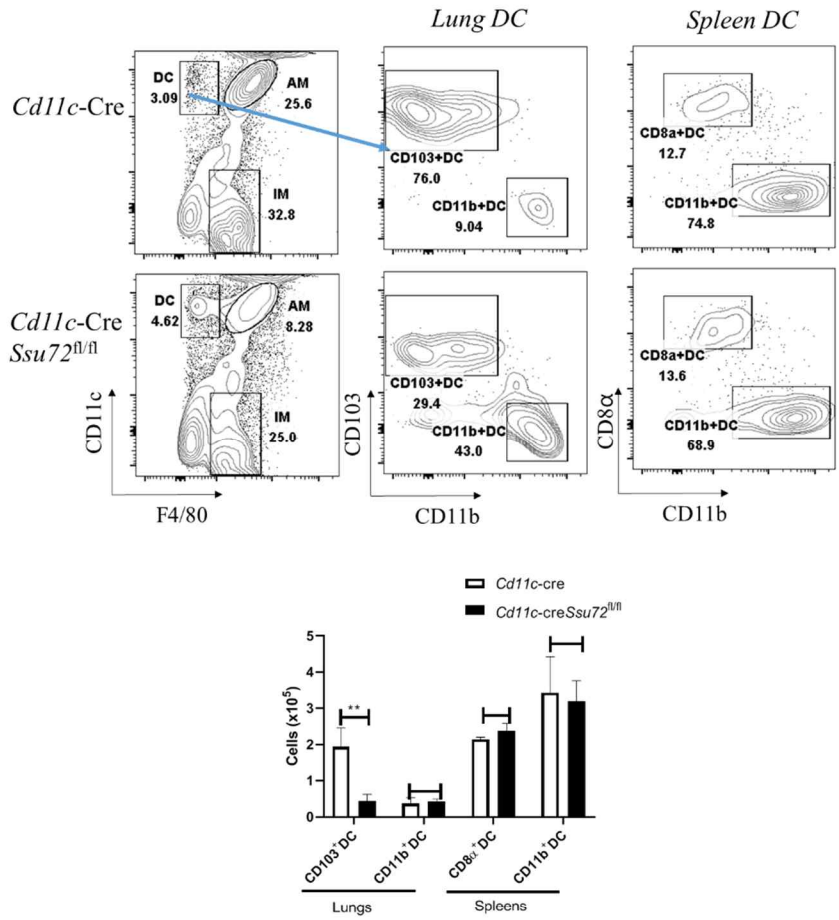
Lung DC
Spleen DC
Cd11c-Cre
DC
3.09
AM
25.6
IM
32.8
CD103+DC
76.0
CD11b+DC
9.04
CD8a+DC
12.7
CD11b+DC
74.8
Cd11c-Cre
Ssu72fl/fl
DC
4.62
AM
8.28
IM
25.0
CD103+DC
29.4
CD11b+DC
43.0
CD8a+DC
13.6
CD11b+DC
68.9
CD11c
F4/80
CD103
CD11b
CD8α
CD11b
Cd11c-cre
Cd11c-creSsu72fl/fl
Cells (x10^5)
CD103+DC
CD11b+DC
CD8α+DC
CD11b+DC
Lungs
Spleens

B

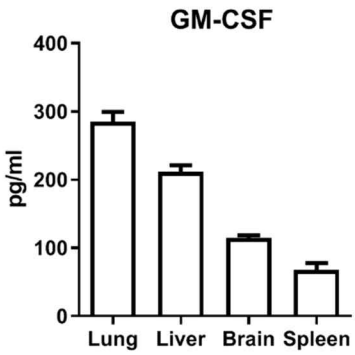
GM-CSF
pg/ml
400
300
200
100
0
Lung
Liver
Brain
Spleen

Figure 13. Ssu72 regulates lung CD103^{+}DCs

(A) Lungs and spleen from *Cd11c*-cre*Ssu72*$^{fl/fl}$ and in *Cd11c*-cre mice were analyzed via flow cytometry. Following markers were used for analysis of DCs – CD103^{+}DC – CD45^{+}CD11c^{+}F4/80^{-}MHC-II^{+}CD103^{+}CD11b^{-}, Lung CD11b^{+}DC – CD45^{+}CD11c^{+}F4/80^{-}MHC-II^{+}CD103^{-}CD11b^{+} CD8α^{+}DC – CD45^{+}CD11c^{+}MHC-II^{+}CD8α^{+}CD11b^{-} Spleen CD11b^{+}DC – CD45^{+}CD11c^{+}MHC-II^{+}CD8α^{-}CD11b^{+}. Absolute cell numbers were estimated by multiplying total numbers of cell obtained from each tissue by percentages of each subset.

(B) WT lungs, livers, brains and spleens were homogenized in 1× PBS and supernatants were used for ELISA of GM-CSF. Using the same supernatants, Bradford assay was conducted to measure total protein concentrations within each tissue. The finalized data is represented per gram of tissue. (A-B; n = 6 per group) Data were pooled from 3 independent experiments and presented as means ± SEMS. Ns, Not significant. *P<0.5, **P<0.01, and ***P<0.001.

Ssu72-mediated fine tuning of GM-CSFR signaling regulates the cellular homeostasis, mitochondrial respiration and functionalities of mature AMs

To address whether down-regulation of enhanced GM-CSFR signaling in Ssu72-deficient mature AMs restores cellular homeostasis, AZD1480, a JAK2 inhibitor was treated to mature AMs from *Lysm*-Cre*Ssu*72$^{fl/fl}$ and *Lysm*-Cre mice, in presence of GM-CSF because JAK2 directly phosphorylates serine and tyrosine residues on GM-CSFRβc. Upon AZD 1480 treatment, numbers, cyclin expressions, cell death in Ssu72-deficient mature AMs were restored similarly to those of WT mature AMs. (Figure 14A&B&C) Similarly, AZD 1480 treatment also restored OCR, mitochondrial ROS, mass and membrane potential, as well as mitochondrial related gene expressions in Ssu72-deficient mature AMs. (Figure 14D&E&F) Lastly, AZD 1480 treatment restored TNF-α production and expression of MHC class II of Ssu72-deficient mature AMs upon LPS treatment and increased FITC staining after incubation with FITC-tagged OVA antigen. (Figure 14G&H&I) Collectively, these results suggest that Ssu72-mediated fine tuning of GM-CSFR signal regulates the cellular homeostasis, mitochondrial respirations as well as functionalities of mature AMs.

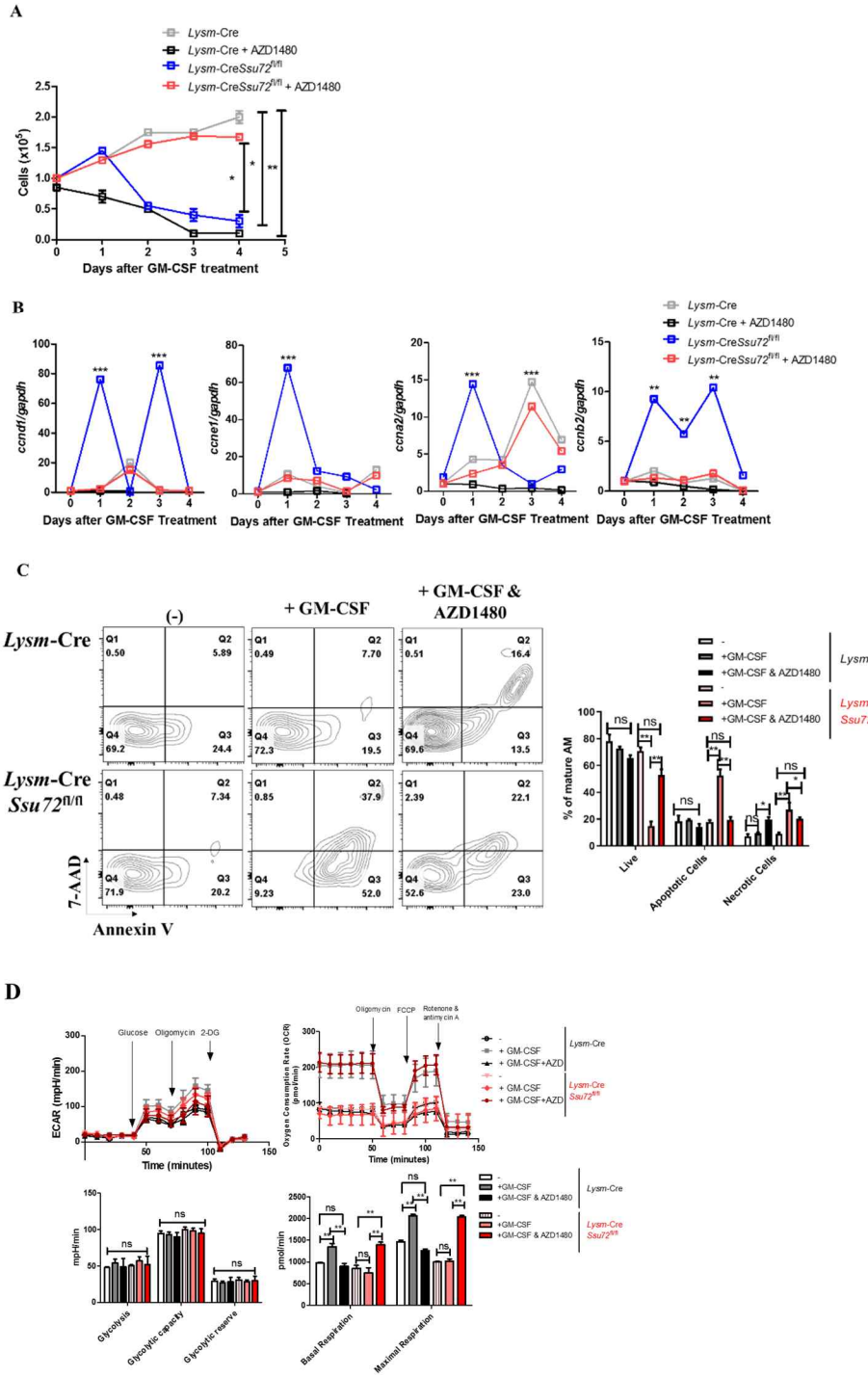
A
Lysm-Cre
Lysm-Cre + AZD1480
Lysm-CreSsu72fl/fl
Lysm-CreSsu72fl/fl + AZD1480
Cells (x10^5)
Days after GM-CSF treatment
B
ccnd1/gapdh
ccne1/gapdh
ccna2/gapdh
ccnb2/gapdh
Days after GM-CSF Treatment
C
(-)
+ GM-CSF
+ GM-CSF & AZD1480
Lysm-Cre
Lysm-Cre Ssu72fl/fl
7-AAD
Annexin V
% of mature AM
Live
Apoptotic Cells
Necrotic Cells
D
Glucose
Oligomycin
2-DG
ECAR (mpH/min)
Time (minutes)
Oligomycin
FCCP
Rotenone & antimycin A
Oxygen Consumption Rate (OCR) (pmol/min)
Glycolysis
Glycolytic capacity
Glycolytic reserve
Basal Respiration
Maximal Respiration

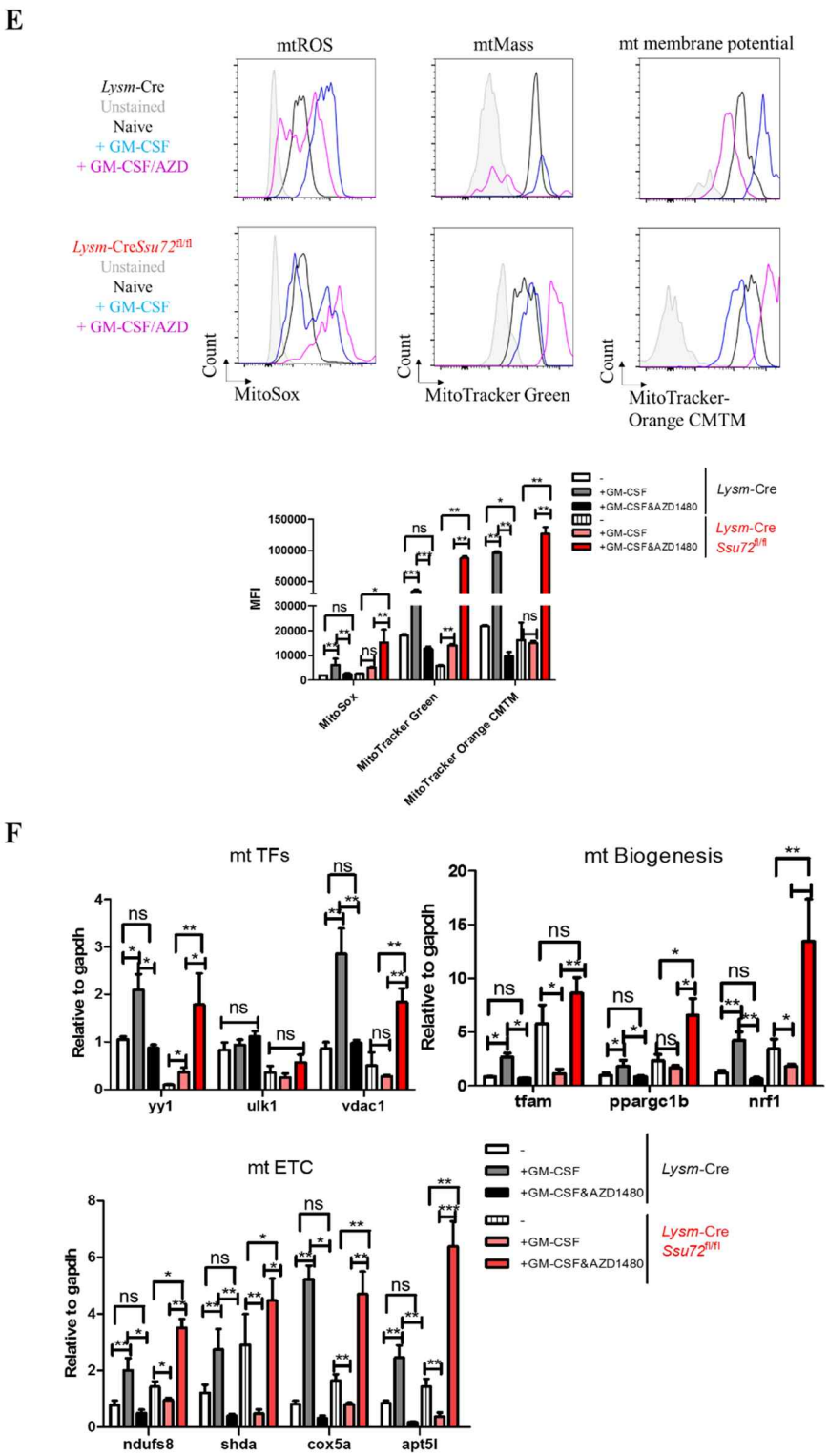
E
mtROS
mtMass
mt membrane potential
Lysm-Cre
Unstained
Naive
+ GM-CSF
+ GM-CSF/AZD
Lysm-CreSsu72fl/fl
Unstained
Naive
+ GM-CSF
+ GM-CSF/AZD
Count
MitoSox
MitoTracker Green
MitoTracker-
Orange CMTM
MFI
-
+GM-CSF
+GM-CSF&AZD1480
Lysm-Cre
Lysm-Cre
Ssu72fl/fl
MitoSox
MitoTracker Green
MitoTracker Orange CMTM
F
mt TFs
mt Biogenesis
Relative to gapdh
yy1
ulk1
vdac1
tfam
ppargc1b
nrf1
mt ETC
ndufs8
shda
cox5a
apt5l
ns

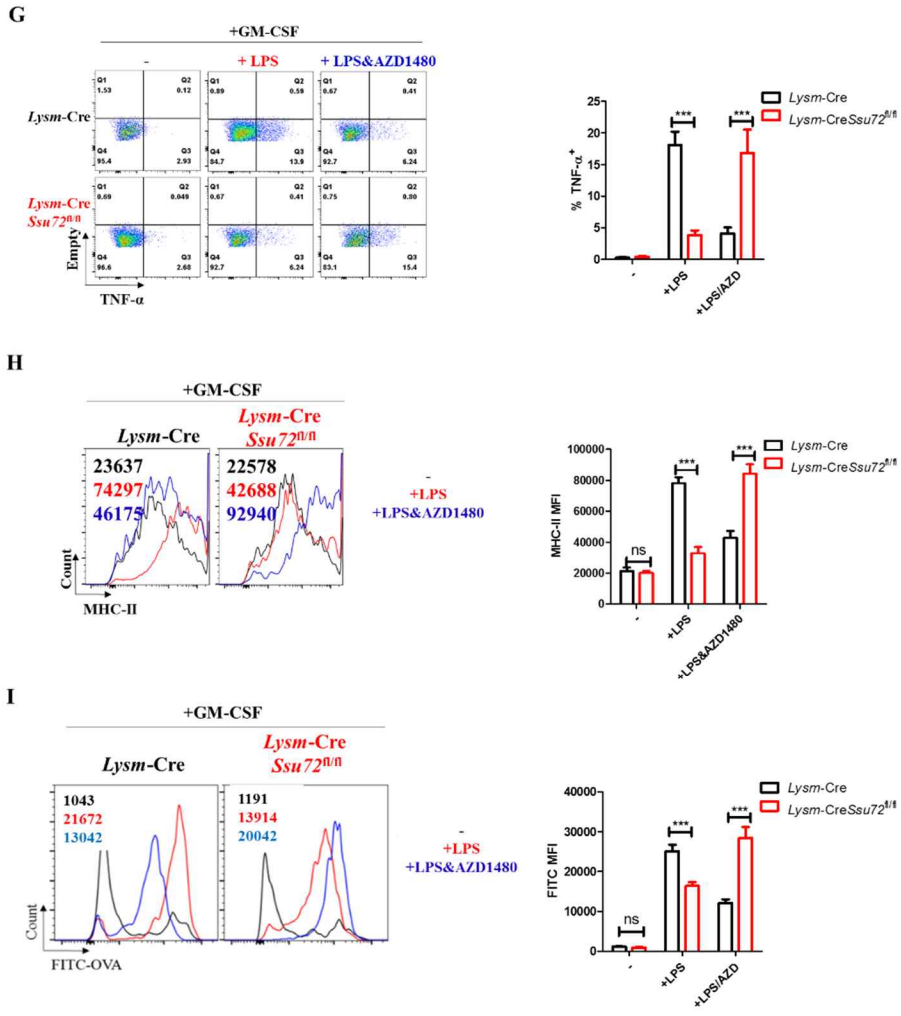
G
+GM-CSF
-
+ LPS
+ LPS&AZD1480
Lysm-Cre
Lysm-Cre Ssu72fl/fl
Empty
TNF-α
% TNF-α+
Lysm-Cre
Lysm-CreSsu72fl/fl
+LPS
+LPS/AZD
H
+GM-CSF
Lysm-Cre
Lysm-Cre Ssu72fl/fl
23637
74297
46175
22578
42688
92940
Count
MHC-II
+LPS
+LPS&AZD1480
MHC-II MFI
ns
I
+GM-CSF
Lysm-Cre
Lysm-Cre Ssu72fl/fl
1043
21672
13042
1191
13914
20042
Count
FITC-OVA
+LPS
+LPS&AZD1480
FITC MFI
ns

Figure 14. Ssu72 mediated fine-tuning of GM-CSFR signaling restores defects found in Ssu72-deficient mature AMs.

(A-F) Sorted mature AMs from *Lysm*-Cre*Ssu*72$^{fl/fl}$ and *Lysm*-Cre mice were treated with GM-CSF (20 ng/ml) and if necessary pre-treated with AZD1480 (2uM) for 2 hr prior to treatment with GM-CSF. (A) Total numbers of mature AMs were counted, (B) cyclin expression were measured via real-time PCR. Expression levels are represented as a fold change over the expression in cells from *Lysm*-Cre*Ssu*72$^{fl/fl}$ mice. (C) Cell death of mature AMs were measured via 7-AAD & Annexin V staining one day after GM-CSF & AZD1480 treatment. (D) Sorted mature AMs were plated in XF24 plate at 2.0x10^5 per well for analysis of ECAR & OCR. Area under the curves were calculated to measure glycolytic capacities as well as mitochondrial respirations. (E) The following reagents were treated with indicated concentrations - MitoSox 1μM, MitoTracker Green 100nM, MitoTracker-Orange CMTM for analysis of mitochondrial ROS, mass and membrane potential respectively. (F) Mitochondria related gene expressions were measured via real-time PCR. Expression levels are represented as a fold change over the expression in cells from *Lysm*-Cre*Ssu*72$^{fl/fl}$ mice. (A-F; n = 16 per group) (G-I) Sorted mature AMs from *Lysm*-Cre*Ssu*72$^{fl/fl}$ and *Lysm*-Cre mice were treated with GM-CSF (20 ng/ml) and if necessary pre-treated with AZD1480 (2uM) for 2 hr prior to treatment with GM-CSF followed by treatment with LPS (100 ng/ml) 4 hrs. (G) TNF-α secreting capacity, (H) MHC-II expression (I) Antigen uptake capacity were measured via flow cytometry. (G-I; n = 16 per group) Data were pooled from 5 independent experiments and presented as means ± SEMS. Ns, Not significant. *P<0.5, **P<0.01, and ***P<0.001.

Ssu72 regulates allergic asthma via fine tuning of GM-CSFR signaling in mature AMs

To explore whether Ssu72 in mature AMs affects the development of respiratory disease such as allergic asthma, *Lysm*-Cre*Ssu72*$^{fl/fl}$ and *Lysm*-Cre mice were challenged with OVA-induced asthma model and tested for their airway resistance and immune responses in the lungs. (Figure15A) *Lysm*-Cre*Ssu72*$^{fl/fl}$ mice showed less airway hyper-responsiveness (AHR) and the numbers of cells in the lungs, bronchial alveolar lavage (BAL), and bronchial lymph nodes (bLNs) than those of *Lysm*-Cre mice. (Figure 16A&B) Lower levels of *gata3*, *il4*, *il13*, and *il17* expression as were found in the lungs of *Lysm*-Cre*Ssu72*$^{fl/fl}$ mice compared to those of *Lysm*-Cre mice, whereas the expression levels of *ifng* and *il10* were similar in the lungs of two mice strains. (Figure16C&D) Consistent with *in-vitro* results, Ssu72-deficient mature AMs displayed much lower MHC-II expression compared with that of WT mature AMs during OVA-induced asthma. (Figure 16E) These findings indicate that Ssu72 in mature AMs affects AHR and immune response in OVA-induced asthma.

To verify this, WT or Ssu72-deficient mature AMs were adoptive transferred into *Lysm*-Cre*Ssu72*$^{fl/fl}$ mice during OVA-induced asthma. WT mature AMs cells restored AHR and cell numbers in the lungs, BAL, and bLNs of *Lysm*-Cre*Ssu72*$^{fl/fl}$ mice, whereas Ssu72-deficient mature

AMs cells did not. *il4*, *il13*, and *il17* levels and transcript of *gata3* and *rorc* were high in *Lysm*-Cre mice and *Lysm*-Cre*Ssu72*$^{fl/fl}$ mice adoptively transferred with WT mature AMs, whereas they were low in *Lysm*-Cre*Ssu72*$^{fl/fl}$ mice and *Lysm*-Cre*Ssu72*$^{fl/fl}$ mice adoptively transferred with Ssu72-deficient mature AMs. (Figure16A&B&C&D) Taken together, these results indicate that Ssu72 in mature AMs regulates allergic asthma via fine tuning of GM-CSFR signaling.

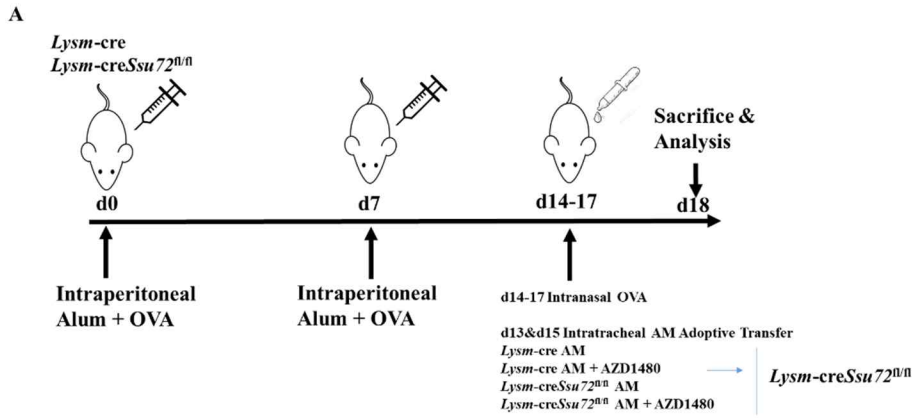

Figure 15. Experimental schematics of OVA-induced asthma and adoptive transfer of AMs.

(A) The details of the experiments are described under "OVA-induced asthma" in material & methods. For adoptive transfer of mature AMs, sorted mature AMs from *Lysm*-Cre and *Lysm*-Cre*Ssu72*$^{fl/fl}$ mice were adoptive transferred into *Lysm*-Cre*Ssu72*$^{fl/fl}$ mice via intratracheal route. Mature AMs were pre-treated with AZD1480 (2μM) for 2 hr prior to transfer into *Lysm*-Cre*Ssu72*$^{fl/fl}$ mice if necessary.

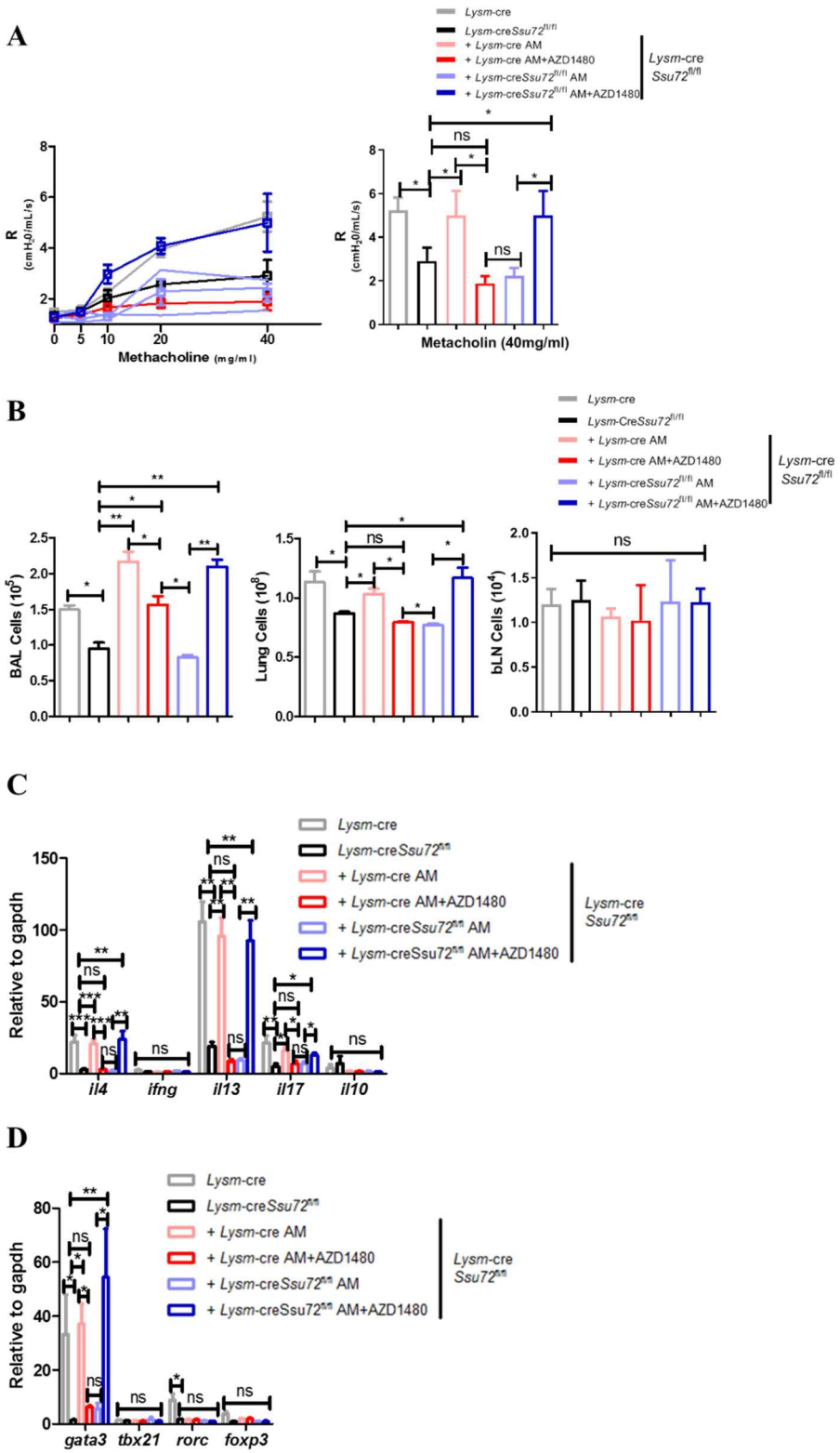
A
Lysm-cre
Lysm-creSsu72fl/fl
+ Lysm-cre AM
+ Lysm-cre AM+AZD1480
+ Lysm-creSsu72fl/fl AM
+ Lysm-creSsu72fl/fl AM+AZD1480
Lysm-cre Ssu72fl/fl
R (cmH2O/mL/s)
Methacholine (mg/ml)
Metacholin (40mg/ml)
B
BAL Cells (10^5)
Lung Cells (10^8)
bLN Cells (10^6)
C
Relative to gapdh
Lysm-cre Ssu72fl/fl
il4
ifng
il13
il17
il10
D
gata3
tbx21
rorc
foxp3

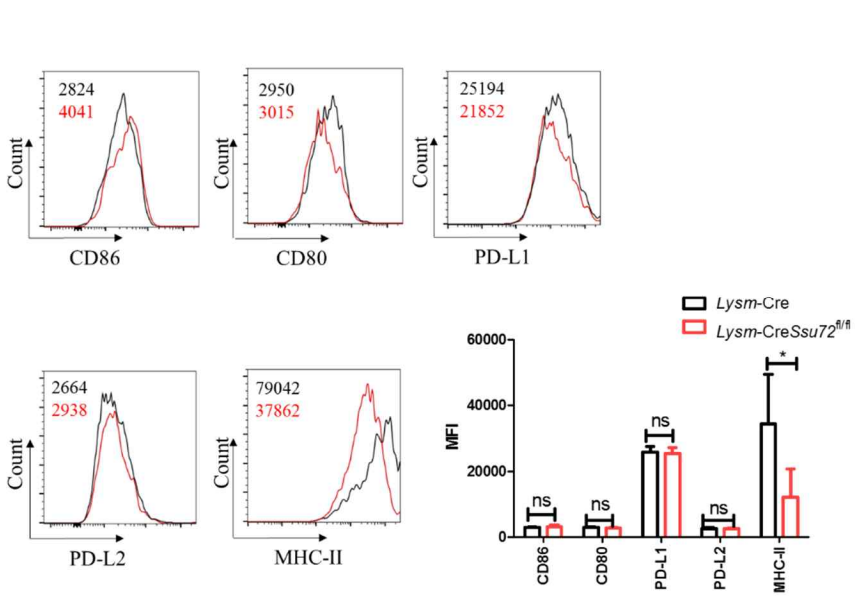

Figure 16. Ssu72 regulates allergic asthma via fine-tuning of GM-CSFR signaling in mature AMs.

(A-D) *Lysm*-Cre mice and *Lysm*-Cre*Ssu72*$^{fl/fl}$ mice or *Lysm*-Cre*Ssu72*$^{fl/fl}$ mice adoptive transferred with WT mature AMs, WT mature AMs pre-treated with AZD1480 (2μM), Ssu72-deficient mature AMs, and Ssu72 deficient mature AMs pre-treated with AZD1480 (2μM) were analyzed for development of allergic asthma. (A) Airway-hyperreactivity (AHR) was measured via flexivent, (B) Total cell numbers in bronchial LNs, BALs and lungs were estimated, (C) The transcript levels of key cytokines were measured in lungs via real-time PCR (D) T cell transcription factor transcript levels were measured in lungs via real-time PCR. For real-time PCR analysis, expression levels are represented as a fold change over the expressions in cells from *Lysm*-Cre*Ssu72*$^{fl/fl}$ mice. (E) Mature AMs from lungs of *Lysm*-Cre and *Lysm*-Cre*Ssu72*$^{fl/fl}$ mice were gated during OVA-induced asthma and expression levels of surface molecules were analyzed via flow cytometry. (A-D; $n = 10$, E; $n = 15$ per

group) Data were pooled from 5 independent experiments and presented as means ± SEMS. Ns, Not significant. *P<0.5, **P<0.01, and ***P<0.001.

DISCUSSION

Ssu72 is a phosphatase that regulates RNA polymerase activity in the nucleus [15, 16]. However, cytosol & nuclear fraction as well as confocal microscopy result show that Ssu72 was expressed at much higher level in cytoplasm rather than in nucleus of AMs, suggesting that Ssu72 might exert phosphatase activity in the cytoplasm as well as in the nucleus. While there is still a possibility of nucleus Ssu72 contributing to regulation of AMs, the fine-tuning experiments using AZD1480 demonstrate that regulation of GM-CSF signaling has contributed significantly in regulation of AMs. Moreover, *Cd11c*-cre*Ssu72*$^{fl/fl}$ mice showed a reduction in numbers and maturational defect of AMs in postnatal period. These phenotypes of AMs in *Lysm*-Cre*Ssu*72$^{fl/fl}$ and *Cd11c*-cre*Ssu72*$^{fl/fl}$ mice are similar to those of GM-CSF and PPAR-γ-deficient mice and emerging evidences have demonstrated that GM-CSFR-PPAR-γ axis is essential for the differentiation and maturation of AMs [9, 10]. Thus, these findings suggest that Ssu72 might be involved in regulation of GM-CSFR-PPAR-γ axis in AMs. Consistently, upon GM-CSF treatment, Ssu72 directly bound to GM-CSFR βc and its expression level was increased in WT AMs. Moreover, GM-CSF stimulation increased phosphorylation of GM-CSFR βc and its downstream

molecules more, but reduced the expression level of *pparg* in Ssu72-deficient AMs compared with that of WT AMs, indicating that Ssu72 regulates GM-CSFR signaling in AMs by reducing GM-CSFR βc phosphorylation. Several studies have demonstrated that GM-CSF-GM-CSFR interaction triggers phosphorylation of two residues of GM-CSFR βc (Ser585 and Tyr577) by JAK2, in turn, which provides binding sites for STAT3 and STAT5, thereby initiating JAK-STAT signaling [29, 30, 31, 32]. However, it is unclear which phosphorylation sites of GM-CSFR βc in AMs is regulated by Ssu72 upon GM-CSF stimulation. In Ssu72-deficient AMs, GM-CSF increased phosphorylation of AKT and ERK as well as Ser and Tyr phosphorylation of GM-CSFR βc. Guthridge et al. demonstrated that Ser585 and Tyr577 phosphorylation of GM-CSFR βc triggers AKT and ERK phosphorylation, respectively [33]. Thus, it is reasonable to consider that Ssu72 regulates the phosphorylation of both Ser585 and Tyr577 in AMs. Combined, these findings indicate that Ssu72 regulates development and maturation of AMs by directly binding to GM-CSFR βc and regulating phosphorylation status of GM-CSFR βc and downstream molecules.

GM-CSFR signaling is regulated via balancing between positive and negative signals at several levels including downregulating of GM-CSFR expression on cell surface, and reversible phosphorylation of

downstream signal molecules, a negative regulator of the GM-CSFR signaling such as Src-like adaptor protein [14]. Moreover, high concentration of GM-CSF induces cellular proliferation, differentiation, and functional activation as well as cell survival via JAK2-mediated phosphorylation of Tyr577 in GM-CSFR βc, whereas Ser585 is phosphorylated at low concentration of GM-CSF, leading to cell survival. These findings indicate that GM-CSF induces various cellular outcomes by providing differential signals in a dose-dependent manner. Based on these findings, it is feasible that fine-tuning of GM-CSFR signaling via phosphorylation of two tyrosine residues is critical for regulating cellular events of AMs. However, there has been no study to report a phosphatase that provides fine-tuning of GM-CSFR signaling by directly binding to GM-CSFR βc. In our experiments, downregulation of phosphorylation levels of GM-CSFR βc using JAK2 inhibitor restored dysregulation of GM-CSF-mediated cell cycle, proliferation, survival and mitochondrial function in Ssu72-deficient mature AMs, indicating that Ssu72 exerts fine-tuning effect on GM-CSFR signaling by negatively regulating phosphorylation of GM-CSFR βc in mature AMs. Nevertheless, it is unclear whether Ssu72-mediated regulation of RNA polymerase II activity also contributes to these cellular events in AMs in addition to fine-tuning effect on GM-CSFR signaling, which might need further investigation.

Consistent with the data presented here, GM-CSF has been known to play a role in myeloid cell survival, proliferation, differentiation, migration, and functional activation [34]. Moreover, recent study reported that GM-CSF increased glycolysis via de novo synthesis of glucose transporters and c-myc in BMDM, indicating that GM-CSF also regulates metabolic reprograming in macrophages [35]. However, it is unclear whether GM-CSFR signaling regulates mitochondrial respiration in AMs. Ssu72-deficient mature AMs showed dysregulation in OCR and mitochondria ROS generation upon GM-CSF stimulation, which was restored by decreasing phosphorylation of GM-CSFR βc using JAK2 inhibitor. These findings indicate that Ssu72-mediated fine tuning GM-CSFR signaling is critical for regulation of mitochondrial respiration in AMs. However, there is lack of understanding between mitochondrial homeostasis in AMs. Recently, it was demonstrated that AMs from patients with chronic obstructive pulmonary disease (COPD) increased basal mROS expression but failed in pneumococcus-induced mROS generation. Moreover, Akt-1-mediated mitophagy is required for TGF-β1 production and apoptosis resistance of AMs, thereby contributing to pulmonary fibrosis. These findings suggest that mitochondria homeostasis in AMs might contribute to the pathogenesis of respiratory diseases. Therefore, it is likely that Ssu72-mediated regulation of mitochondria homeostasis might be involved in respiratory

diseases.

In addition to dysregulation of cellular homeostasis and mitochondria, Ssu72-deficient AMs showed a defect in TNF-α production and expression of MHC-II upon LPS stimulation, and antigen uptake capacity. These findings suggest that Ssu72-mediated fine tuning of GM-CSFR signaling in AMs might be involved in the regulation of respiratory diseases including asthma. However, the function of AMs in asthma has been widely contradictory, depending on stage of inflammation and ontogeny of macrophages[36]. Nevertheless, ova-induced asthma experiments demonstrated that Ssu72-deficient AMs failed to induce AHR and Th2 responses in the lungs during OVA-induced asthma, which was restored by transferring Ssu72-deficient AMs treated with AZD 1480. These findings indicate that Ssu72-mediated fine tuning of GM-CSFR signaling is critical for AMs in allergic asthma.

In conclusion, these data suggest that Ssu72 binds to and regulates phosphorylation of GM-CSFR βc, thereby providing fine-tuning of GM-CSFR signaling in AMs, which contributes to the development and maturation of AMs, and prevention of asthma altogether. (Figure 17)

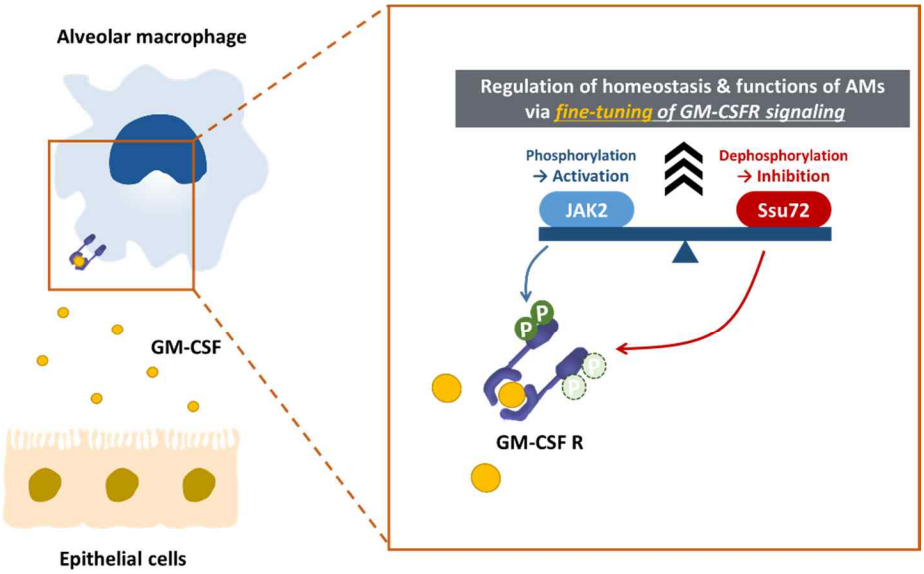

Figure 17. Graphical abstract of Ssu72 mediated fine-tuning of GM-CSFR signaling in AMs.

REFERENCES

1. Sieweke, M.H. & Allen, J.E. Beyond stem cells: self-renewal of differentiated macrophages. *Science* **342**, 1242974 (2013).

2. Hashimoto, D. *et al.* Tissue-resident macrophages self-maintain locally throughout adult life with minimal contribution from circulating monocytes. *Immunity* **38**, 792-804 (2013).

3. Bajpai, G. *et al.* Tissue Resident CCR2- and CCR2+ Cardiac Macrophages Differentially Orchestrate Monocyte Recruitment and Fate Specification Following Myocardial Injury. *Circ Res* **124**, 263-278 (2019).

4. Liao, X. *et al.* Distinct roles of resident and nonresident macrophages in nonischemic cardiomyopathy. *Proc Natl Acad Sci U S A* **115**, E4661-E4669 (2018).

5. Dick, S.A. *et al.* Self-renewing resident cardiac macrophages limit adverse remodeling following myocardial infarction. *Nat Immunol* **20**, 29-39 (2019).

6. Gautier, E.L. *et al.* Gene-expression profiles and transcriptional regulatory pathways that underlie the identity and diversity of mouse tissue macrophages. *Nat Immunol* **13**, 1118-1128 (2012).

7. Soucie, E.L. *et al.* Lineage-specific enhancers activate self-renewal genes in macrophages and embryonic stem cells. *Science* **351**, aad5510 (2016).

8. Kurotaki, D., Sasaki, H. & Tamura, T. Transcriptional control of monocyte and macrophage development. *Int Immunol* **29**, 97-107 (2017).

9. Guilliams, M. *et al.* Alveolar macrophages develop from fetal monocytes that differentiate into long-lived cells in the first week of life via GM-CSF. *J Exp Med* **210**, 1977-1992 (2013).

10. Schneider, C. *et al.* Induction of the nuclear receptor PPAR-gamma by the cytokine GM-CSF is critical for the differentiation of fetal monocytes into alveolar macrophages. *Nat Immunol* **15**, 1026-1037 (2014).

11. Shibata, Y. *et al.* GM-CSF regulates alveolar macrophage differentiation and innate immunity in the lung through PU.1. *Immunity* **15**, 557-567 (2001).

12. Huffman Reed, J.A. *et al.* GM-CSF enhances lung growth and causes alveolar type II epithelial cell hyperplasia in transgenic mice. *The American journal of physiology* **273**, L715-725 (1997).

13. Guthridge, M.A. *et al.* Growth factor pleiotropy is controlled by a receptor Tyr/Ser motif that acts as a binary switch. *The EMBO journal* **25**, 479-489 (2006).

14. Liontos, L.M. *et al.* The Src-like adaptor protein regulates GM-CSFR signaling and monocytic dendritic cell maturation. *J Immunol* **186**, 1923-1933 (2011).

15. Dichtl, B. *et al.* A role for SSU72 in balancing RNA polymerase II transcription elongation and termination. *Molecular cell* **10**, 1139-1150 (2002).

16. Hsin, J.P. & Manley, J.L. The RNA polymerase II CTD coordinates transcription and RNA processing. *Genes Dev* **26**, 2119-2137 (2012).

17. Kim, H.S. *et al.* Functional interplay between Aurora B kinase and Ssu72 phosphatase regulates sister chromatid cohesion. *Nature communications* **4**, 2631 (2013).

18. Lee, S.H. *et al.* Ssu72 attenuates autoimmune arthritis via targeting of STAT3 signaling and Th17 activation. *Sci Rep* **7**, 5506 (2017).

19. Weischenfeldt, J. & Porse, B. Bone Marrow-Derived Macrophages (BMM): Isolation and Applications. *CSH Protoc* **2008**, pdb prot5080 (2008).

20. Suzuki, T. & Trapnell, B.C. Pulmonary Alveolar Proteinosis Syndrome. *Clin Chest Med* **37**, 431-440 (2016).

21. Duan, W. & Croft, M. Control of regulatory T cells and airway tolerance by lung macrophages and dendritic cells. *Ann Am Thorac Soc* **11 Suppl 5**, S306-313 (2014).

22. Hoeffel, G. & Ginhoux, F. Ontogeny of Tissue-Resident Macrophages. *Front Immunol* **6**, 486 (2015).

23. Baumann, K. Cell cycle: Cyclin A corrections. *Nat Rev Mol Cell Biol* **14**, 692 (2013).

24. Lambrecht, B.N. Alveolar macrophage in the driver's seat. *Immunity* **24**, 366-368 (2006).

25. Willems, P.H., Rossignol, R., Dieteren, C.E., Murphy, M.P. & Koopman, W.J. Redox Homeostasis and Mitochondrial Dynamics. *Cell Metab* **22**, 207-218 (2015).

26. Reichart, G. *et al.* Mitochondrial complex IV mutation increases reactive oxygen species production and reduces lifespan in aged mice. *Acta Physiol (Oxf)* **225**, e13214 (2019).

27. McClure, B.J. *et al.* Molecular assembly of the ternary granulocyte-macrophage colony-stimulating factor receptor complex. *Blood* **101**, 1308-1315 (2003).

28. Greter, M. *et al.* GM-CSF controls nonlymphoid tissue dendritic cell homeostasis but is dispensable for the differentiation of inflammatory dendritic cells. *Immunity* **36**, 1031-1046 (2012).

29. Hansen, G. *et al.* The structure of the GM-CSF receptor

complex reveals a distinct mode of cytokine receptor activation. *Cell* **134**, 496-507 (2008).

30. Hercus, T.R. *et al.* Signalling by the betac family of cytokines. *Cytokine & growth factor reviews* **24**, 189-201 (2013).

31. Ramshaw, H.S. *et al.* The Shc-binding site of the betac subunit of the GM-CSF/IL-3/IL-5 receptors is a negative regulator of hematopoiesis. *Blood* **110**, 3582-3590 (2007).

32. Guthridge, M.A. *et al.* Site-specific serine phosphorylation of the IL-3 receptor is required for hemopoietic cell survival. *Molecular cell* **6**, 99-108 (2000).

33. Guthridge, M.A. *et al.* The phosphoserine-585-dependent pathway of the GM-CSF/IL-3/IL-5 receptors mediates hematopoietic cell survival through activation of NF-kappaB and induction of bcl-2. *Blood* **103**, 820-827 (2004).

34. Broughton, S.E. *et al.* The betac receptor family - Structural insights and their functional implications. *Cytokine* **74**, 247-258 (2015).

35. Na, Y.R. *et al.* GM-CSF Induces Inflammatory Macrophages by Regulating Glycolysis and Lipid Metabolism. *J Immunol* **197**, 4101-4109 (2016).

36. Lumeng, C.N. Lung Macrophage Diversity and Asthma. *Annals of the American Thoracic Society* **13 Suppl 1**, S31-34 (2016).

국문 초록

Ssu72는 탈인산가수분해효소로써, 리보핵산중합효소-II의 인산화 정도 및 활성화를 조절하는 단백으로 잘 알려져 있다. 하지만, Ssu72가 대식세포에 미치는 영향에 대한 보고는 전무하다. 이 연구는 Ssu72가 폐포대식세포의 GM-CSF 신호전달체계에 관여하여 폐포대식세포의 항상성 및 기능에 관여함을 규명하였다. 폐포대식세포에 GM-CSF 자극이 주어졌을 시, Ssu72는 GM-CSF 수용체 베타체인과 결합하고 그 인산화 정도를 조절하여 GM-CSF 신호전달 체계를 조절함을 확인하였고, 따라서 Ssu72가 결핍된 폐포대식세포는 정상 폐포대식세포에 비교해 세포주기, 사멸, 증식 그리고 미토콘드리아 호흡에 문제가 발생함을 확인하였다. 더 나아가, Ssu72가 결핍된 폐포대식세포에 GM-CSF 수용체의 베타체인의 인산화를 담당하고 있는 JAK2에 대한 억제제 처리를 통해 GM-CSF 신호전달 체계를 회복시켰을 시 비정상적인 세포 항상성이 정상화 되는 것을 확인하였다. 또한, *Lysm*-Cre*Ssu72*$^{fl/fl}$ 마우스는 생후직후부터 폐포대식세포의 발달 및 성장 그리고 기능에 문제가 발생하여 있음을

확인하였고, 이는 알레르기성 천식을 억제함을 확인하였다. 특히, Ssu72 결핍 폐포대식세포에 JAK2 억제제 처리 시 천식의 발병률이 다시 증가함을 확인하였다. 따라서, 이 연구 결과들은 GM-CSF 신호전달 체계가 Ssu72에 의해 미세조정 되고 있고, Ssu72가 GM-CSF 수용체 베타체인과 결합함으로써 폐포대식세포의 발달 및 성장 그리고 기능에 관여함을 규명하였다.

주요어 : Ssu72, 폐포대식세포, GM-CSF, 미세조정

학번 : 2013-21780